

Summer 8-18-2015

Temperature as a Proxy to Study the Flow of Water Within Two Maine Streambeds

Jarrold D. Cicha

University of Maine - Main, jarrod.cicha@maine.edu

Follow this and additional works at: <http://digitalcommons.library.umaine.edu/etd>

 Part of the [Hydrology Commons](#)

Recommended Citation

Cicha, Jarrod D., "Temperature as a Proxy to Study the Flow of Water Within Two Maine Streambeds" (2015). *Electronic Theses and Dissertations*. 2353.

<http://digitalcommons.library.umaine.edu/etd/2353>

This Open-Access Thesis is brought to you for free and open access by DigitalCommons@UMaine. It has been accepted for inclusion in Electronic Theses and Dissertations by an authorized administrator of DigitalCommons@UMaine.

**TEMPERATURE AS A PROXY TO STUDY THE
FLOW OF WATER WITHIN TWO
MAINE STREAMBEDS**

By

Jarrold Cicha

B.A. University of Minnesota Morris, 2009

A THESIS

Submitted in Partial Fulfillment of the

Requirements for the Degree of

Master of Science

(in Earth and Climate Sciences)

The Graduate School

The University of Maine

August 2015

Advisory Committee:

Andrew Reeve, Professor of Earth and Climate Sciences, Advisor

Sean Smith, Assistant Professor of Earth and Climate Sciences

Amanda Olsen, Assistant Professor of Earth and Climate Sciences

**TEMPERATURE AS A PROXY TO STUDY THE
FLOW OF WATER WITHIN TWO
MAINE STREAMBEDS**

By

Jarrold Cicha

B.A. University of Minnesota Morris, 2009

A THESIS

Submitted in Partial Fulfillment of the

Requirements for the Degree of

Master of Science

(in Earth and Climate Sciences)

The Graduate School

The University of Maine

August 2015

Advisory Committee:

Andrew Reeve, Professor of Earth and Climate Sciences, Advisor

Sean Smith, Assistant Professor of Earth and Climate Sciences

Amanda Olsen, Assistant Professor of Earth and Climate Sciences

THESIS ACCEPTANCE STATEMENT

On behalf of the Graduate Committee for Jarrod Cicha, I affirm that this manuscript is the final and accepted thesis. Signatures of all committee members are on file with the Graduate School at the University of Maine, 42 Stodder Hall, Orono, Maine.

Dr. Andrew Reeve, Professor

Date

LIBRARY RIGHTS STATEMENT

In presenting this thesis in partial fulfillment of the requirements for an advanced degree at The University of Maine, I agree that the Library shall make it freely available for inspection. I further agree that permission for “fair use” copying of this thesis for scholarly purposes may be granted by the Librarian. It is understood that any copying or publication of this thesis for financial gain shall not be allowed without my written permission.

Signature:

Date:

**TEMPERATURE AS A PROXY TO STUDY THE
FLOW OF WATER WITHIN TWO
MAINE STREAMBEDS**

By: Jarrod Cicha

Thesis Advisor: Dr. Andrew Reeve

An Abstract of the Thesis Presented
in Partial Fulfillment of the Requirements for the
Degree of Master of Science
(in Earth and Climate Sciences)
August 2015

Heat transport studies often focus on calculating an average direction and magnitude of groundwater flow within the streambed for long (3 days – 1 week) periods of time. Short-term changes in flow magnitude and/or direction within the streambed caused by near stream groundwater pumping and storms are not represented by these long term averaging methods. Temperature profiles collected in B Stream (Houlton, Maine) and the Stillwater River (Orono, Maine) were used to calibrate a one-dimensional heat transport model and quantify short-term hydraulic events in vertical groundwater velocity within streambeds. Temperature profiles were collected during the summer of 2014 with iButton (Maxim Integrated, San Jose, CA) temperature loggers from two locations within each streambed to assess the spatial variability of groundwater flow within the streambed. Velocity values were averaged over daily periods allowing us to analyze how groundwater flow within the streambed changed during short-term hydraulic events. Bedrock wells at the B Stream site and surficial wells at the Stillwater River site were pumped while streambed temperature profiles were being collected. Temperature profiles were also collected before, during, and after Hurricane Arthur. Average modeled

velocities were -4.38×10^{-6} m/s and -5.01×10^{-6} m/s (standard deviations of 8.02×10^{-6} m/s and 1.34×10^{-5} m/s) for the south and north locations at the Stillwater River site and were -1.13×10^{-5} m/s and -1.93×10^{-5} m/s (standard deviations of 1.46×10^{-5} m/s and 2.03×10^{-5} m/s) for locations 1 and 2 at the B Stream site. Significant ($p = 0.0004$) differences between location 1 and location 2 at the B Stream site were recorded while there is no significant ($p = 0.64$) difference between the north and south locations at the Stillwater River site. Model results indicate periods of directional change of groundwater flow at both study sites associated with short-term hydraulic events. Shifts within the Stillwater River are coincident with groundwater pumping while shifts within B Stream are coincident with storm events. Flow within the Stillwater streambed shifts from downward to upward as groundwater wells are turned off at the Stillwater location. Flow within the B Stream streambed shift from downward, to upward, then back to downward. Calculating average velocity over 24 hour time periods allowed for the detection of these changes in the direction of groundwater flow within the streambed.

ACKNOWLEDGMENTS

There are many people who contributed to the completion of my Masters Thesis. Thank you, Joseph Abbot of the Old Town Water District and John Clark of the Houlton Water District, for allowing access to and providing pertinent information about the field sites used in this study. Thank you, Dr. Andrew Reeve, my advisor, for giving me a chance and accepting me as his student. Also, I would like to thank Dr. Reeve for his guidance, cooperation, and patience during this process. Thank you, Dr. Sean Smith and Dr. Amanda Olsen for their insightful comments and edits. Thank you, David Lemery, for providing excellent help in the field and in the lab.

This thesis would not have been possible without the moral support of my fellow graduate student peers and friends (Agnes, Annie, Brett, Brian, Colin, Connor, Cory, and Kara). I cannot express how much I needed your help! I would like to thank Josie for her support and patience through this process, it was a lot of work but I could not have done it without you. I also need to thank Cricket for continuous comic relief and an unlimited amount of snuggles and walks. Last but not least I need to thank my family. Thank you, Mom and Dad, for providing me with the best childhood anybody could ask for and instilling the love of the natural world in me. Thank you, Olivia and Calvin, for being my partners in crime.

TABLE OF CONTENTS

ACKNOWLEDGMENTS iii

LIST OF TABLES vi

LIST OF FIGURES vii

LIST OF SYMBOLS ix

LIST OF EQUATIONS x

CHAPTER 1: INTRODUCTION 1

 1.1 Significance..... 1

 1.2 Measuring Flow Within the Streambed 2

 1.3 Heat Transport and Streambed Variability 6

 1.4 Research Goals and Hypothesis..... 7

CHAPTER 2: SITE DESCRIPTIONS 8

CHAPTER 3: METHODS 13

 3.1 Temperature Time Series Data 13

 3.2 Pumping Tests..... 15

 3.3 One-Dimensional Finite Difference Heat Transport Model 16

CHAPTER 4: RESULTS 20

 4.1 Pumping Tests..... 20

 4.2 Temperature Data..... 20

 4.3 Model Data..... 22

CHAPTER 5: DISCUSSION.....	28
5.1 Pumping Influence on Velocities.....	28
5.2 Storm Event Influence on Velocities	32
5.3 Variance Between Temperatures and Velocities	35
CHAPTER 6: CONCLUSION	39
REFERENCES	40
APPENDIX A: PYTHON SCRIPTS.....	46
APPENDIX B: VELOCITY STATISTICS.....	51
BIOGRAPHY OF THE AUTHOR.....	63

LIST OF TABLES

TABLE 1: Model Parameter Values Used In Simulations.....	17
TABLE 2: Stillwater Velocity Statistics At The North Location	51
TABLE 3: Stillwater Velocity Statistics At The South Location	54
TABLE 4: B Stream Velocity Statistics At Location 1	57
TABLE 5: B Stream Velocity Statistics At Location 2	60

LIST OF FIGURES

FIGURE 1: Map Of The B Stream Field Site.....	11
FIGURE 2: Map Of Stillwater River Site.....	12
FIGURE 3: Ibuttons And Deployment Stick	13
FIGURE 4: Ibuttons Deployed At The B Stream Site.....	14
FIGURE 5: Varying Velocity Within The Model	19
FIGURE 6: Measured Temperature Profile.....	21
FIGURE 7: B Stream Temperatures During Hurricane Arthur	22
FIGURE 8: Average Velocities At Location 1 Of The B Stream Site	24
FIGURE 9: Average Velocities At Location 2 Of The B Stream Site	25
FIGURE 10: Average Velocities At South Location Of The Stillwater River.....	26
FIGURE 11: Average Velocities At North Location Of The Stillwater River.....	27
FIGURE 12: Average Velocities During June Pumping Test At B Stream	29
FIGURE 13: Average Velocities Vs. Pumping Rates At B Stream	31
FIGURE 14: Average Velocities Vs. Stream Stage And Precipitation At B Stream	33
FIGURE 15: Average Velocities Vs. Stream Stage And Precipitation At The Stillwater River	34
FIGURE 16: Average Temperatures At Both Locations Of The B Stream Site	37

FIGURE 17: Average Temperatures At Both Locations At The Stillwater

River Site 38

LIST OF SYMBOLS

T = Temperature

x = distance

t = time

K_t = Energy Storage Constant

K_{CD} = Conduction and Dispersion Constant

K_v = Advection Constant

D = Hydrodynamic Dispersion

k_f = heat conduction of the fluid

k_s = heat conduction of the solid

n = porosity

c_f = heat capacity of the fluid

c_s = heat capacity of the solid

v = velocity of flow

ρ_f = density of the fluid

ρ_s = density of the solid

∂ = partial derivative of following parameter

Δ = delta (change in)

d = change in following parameter

LIST OF EQUATIONS

$$K_t \frac{\partial T}{\partial t} = K_{CD} \cdot \frac{\partial^2 T}{\partial x^2} - K_v \cdot v \cdot \frac{\partial T}{\partial x} \quad (1)$$

$$K_{CD} = (n \cdot k_f + (1-n) \cdot k_s) + n \cdot D \quad (2)$$

$$K_t = \rho_f \cdot c_f \cdot n + (1-n) \cdot \rho_s \cdot c_s \quad (3)$$

$$K_v = n \cdot \rho_f \cdot c_f \quad (4)$$

$$\frac{\partial T}{\partial x} \approx \frac{T_{front} - T_{back}}{\Delta x} \quad (5)$$

$$\frac{v \cdot dt}{dx} < 1 \quad (6)$$

$$R_{NSS} = \frac{\sum_{i=1}^n (T_{i_meas} - T_{i_sim})^2}{n} \quad (7)$$

CHAPTER 1: INTRODUCTION

1.1 Significance

Groundwater and surface water are interconnected resources and the interactions between the two shape the ecosystem around them. Hyporheic exchange, the temporary diversion of surface water into the streambed, is an important process occurring within the streambed (Brunke and Gonser, 1997). Hyporheic exchange can add nutrients and organic matter to the stream and dissolved oxygen to the streambed (Zimmer and Lautz, 2014). Hydrologic events such as groundwater pumping or storms (precipitation runoff events) can change how groundwater and surface water interact. Multiple studies have linked near stream groundwater extraction to the reduction of flow from the groundwater into the surface water (Alley et al., 1999; Dudley and Stewart, 2007; Zume and Tarhule, 2007; Barlow and Leake 2012; Rugel et al., 2012). Alley et al. (1999) and Heath (1983) have shown that the drawdown of the water table caused by pumping a well can change the hydraulic gradient near a surface body of water (Alley et al., 1999; Heath, 1983). This change in gradient can cause an increase in groundwater recharge or decrease in discharge into the stream from the groundwater system (Alley et al., 1999; Dudley and Stewart, 2007; Rugel et al., 2012; Zume and Tarhule, 2007). Zume and Tarhule (2007) used MODFLOW (McDonald and Harbaugh, 1988) to evaluate the impacts of groundwater exploitation on stream flow depletion. Zume and Tarhule's (2007) simulations showed that groundwater pumping reduced baseflow by 29% and increased downward flow of water within the streambed by 18% in the Beaver-North Canadian River in Oklahoma. Rugel et al. (2012) used flow duration curves and annual baseflow recession slopes to describe changes in stream flows caused by agricultural irrigation

systems within the Flint River Basin in southwestern Georgia. Rugel et al. (2012) found substantial reductions in stream baseflow and intensified low-flow and no-flow periods after the irrigation systems were installed.

Storm events and variations in surface discharge have also been shown to alter the flow of groundwater within the streambed (Malcolm et al., 2004; Westhoff et al., 2011; Zimmer and Lautz, 2014). Malcolm et al. (2004) collected high-resolution hydraulic head data and indicated hydrological events (storms) drive rapid changes in flow within streambeds. Malcolm et al. (2004) also observed changes in the hydrochemistry of hyporheic water during these events. Westhoff et al. (2011) used an advection-dispersion model coupled with an energy balance model to simulate in-stream water temperature. Westhoff et al. (2011) showed that infiltration losses were increased during small rain events and that hyporheic exchange varies with varying discharge at the beginning of first order streams.

1.2 Measuring Flow Within the Streambed

Tracing heat signals throughout streambeds has been found to be a useful method for quantifying the movement of water between the groundwater and surface water (Anderson, 2005; Kalbus et al., 2006; Keery et al., 2007). Suzuki (1960) was the first to develop an analytical method that used heat as a tracer to estimate vertical flow. Suzuki (1960) noted that characteristic sinusoidal temperature variations at the surface of the earth are damped with depth below the streambed. He developed a method that used a heat flow equation to estimate vertical one-dimensional groundwater flow by comparing the temperature oscillations at the surface with those at a known depth below the surface (Suzuki, 1960). Stallman (1965) improved upon Suzuki's work and eliminated an

approximation used in Suzuki's method by developing an exact mathematical solution to Suzuki's (1960) work. The transport of heat in the subsurface is a combination of conductive heat transport through the sediments and fluids, the dispersion of the heat due to groundwater velocity variation, and advective heat transport from flowing groundwater. Parameters that quantify the movement of heat in the subsurface can be estimated by fitting temperature profiles recorded within a streambed to an analytic or numerical heat transport model. This is often done by analyzing the damping of the diurnal temperature fluctuation with depth, and the shift in the phase of the temperature signal with depth (Keery et al., 2007; Lautz, 2010; Silliman et al., 1995). These methods fit temperature (T) data measured at a range of (x) and times (t) to the one dimensional heat transport equation (equation 1) with assigned values for a heat energy storage constant (K_t), heat conduction and water dispersion constant (K_{CD}), and advection constant (K_v) (Kipp, 1987). These constants are calculated from the thermal dispersion (D), heat conduction of the water and solid phases (k_f , k_s), porosity (n), heat capacity for the water and solid phases (c_f , c_s), density of the water and solid phases (ρ_f , ρ_s), and vertical groundwater velocity (v).

$$K_t \frac{\partial T}{\partial t} = K_{cd} \cdot \frac{\partial^2 T}{\partial x^2} - K_v \cdot v \cdot \frac{\partial T}{\partial x} \quad (1)$$

$$K_{cd} = (n \cdot k_f + (1 - n) \cdot k_s) + n \cdot D \quad (2)$$

$$K_t = \rho_f \cdot c_f \cdot n + (1 - n) \cdot \rho_s \cdot c_s \quad (3)$$

$$K_v = n \cdot \rho_f \cdot c_f \quad (4)$$

Several studies suggest that thermal dispersion is negligible (Bear, 1972; Ingebritsen and Sanford, 1999; Hopmans et al., 2002). Bravo et al. (2002) imply that thermal dispersion is negligible in the wetland system they investigated and only briefly mention this parameter in their discussion of heat transport applied to wetland systems. Roshan et al. 2012 created a power law relation between D and velocity that is applicable for higher dimensionless anisotropic thermal Peclet numbers (above about 2). Below this threshold, the thermal conductivity of the water and solid are the dominant terms in equation 3, and the assumption that thermal dispersion is negligible becomes valid. This transition occurs at velocities of approximately $3 \times 10^{-4} \text{ m/sec}$ for heat transport through fine sand (Rau et al., 2012). The 1-D heat transport method is only sensitive to thermal diffusion and heat capacity when velocities are low (upflow less than $1.6 \times 10^{-8} \text{ m/sec}$) (Vandenbohede and Lebbe, 2010). Similar results were obtained using forward modeling to assess heat transport (Goto et al., 2005).

Heat transport studies often focus on calculating an average direction and magnitude of groundwater flow within the streambed for long (3 days – 1 week) periods of time (Hatch et al., 2006; Lautz, 2010; Silliman et al., 1995). Short-term changes in flow within the streambed caused by pumping or storms will not be represented by these long term averaging methods. Therefore, it is not possible to fully understand how the flow between the groundwater and surface water is altered during short term events.

Other methods, such as aerial infrared photography, dyes, seepage meters, and stream flow measurements can all be used to quantify the vertical flow of water within streambeds (Kalbus et al., 2006; LaBaugh et al., 2008). Traditional methods for quantifying SBF and hyporheic exchange, such as seepage meters and Darcy flux estimates, have several limitations (Keery et al., 2007). Seepage meters are inexpensive but record average discharge during the entire deployment period. This would prevent the detection of changes in flow during short-term events. There is often uncertainty in Darcy flux methods caused by the large variation in magnitude of the hydraulic properties within a streambed (Keery et al., 2007). Heat transport methods avoid this problem as the properties of water, including density, heat capacity, and heat conductivity are well known and the heat capacity and heat conductivity of naturally occurring solids span a small range of values and can be taken from literature values (Constantz, 2008). Typically, porosity is either measured from sediment samples or estimated based on literature values for the materials observed in the streambed. Temperature data are also a relatively inexpensive parameter to measure and are quick and easy to collect with the emergence of low-cost data-logging temperature sensors (Kalbus et al., 2006).

There are models that couple groundwater flow and heat transport, including HST3D (Kipp, 1987) and VS2DH (Healy and Ronan, 1996), that both numerically solve the 2 or 3 dimensional heat transport equations using the finite difference methods. However, these complex models are not always needed as one-dimensional models can provide accurate high-resolution spatial and temporal data (Hatch et al., 2006; Lautz, 2010). Assumptions of a one-dimensional heat flow models, such as completely vertical flow, are often inconsistently valid in field conditions and have been the focus of multiple

recent studies (Briggs et al., 2013; Cuthbert and Mackay, 2013; Ferguson and Bense, 2011; Lautz, 2010). Lautz (2010) found that errors in vertical flow are small (<20%) when vertical velocities are greater than horizontal velocities. Cuthbert and Mackay (2013) found that strong convergence or divergence of flow introduced significant error in vertical velocities calculated using heat transport methods. However, the errors estimated in this study are relatively small, especially for temperature measurements collected at a depth of 0.1 m (Cuthbert and Mackay, 2013). Ferguson and Bense (2011) found that one-dimensional analytical solutions can provide estimates of specific discharge into streams for specific discharges between 1.0×10^{-7} and 1.0×10^{-5} m/s. However, these estimations are only accurate when the variance in streambed hydraulic conductivity is low (Ferguson and Bense, 2011). Additional information on the application of heat transport methods can be found in Rau et al. (2014).

1.3 Heat Transport and Streambed Variability

The flow of groundwater within streambed has been shown to vary over space and time (Krause et al., 2007; Ellis et al., 2006). Many studies have used heat transport methods to investigate the variability of flow within streambeds (Ferguson and Bense, 2011; Kalbus et al., 2009; Conant, 2004). Conant (2004) related streambed flux obtained from minipiezometer data to streambed temperature and used this relation to Calculate fluxes in a 60 m section of the Pine River in Angus, Ontario, Canada. Kalbus et al. (2009) used a heat transport model to investigate the influence of aquifer and streambed homogeneity on variation of flow within the streambed. Kalbus et al. (2009) found that the homogeneity of the aquifer has a stronger influence on the groundwater fluxes through the streambed than the streambed itself. However, a homogeneous streambed with low hydraulic conductivity resulted in homogenization of fluxes (Kalbus et al.,

2009). Ferguson and Bense (2011) suggests that point measurements made with vertical temperature arrays represent average groundwater velocity over scales of square decimeters to square meters due to temperature averaging resulting from lateral conduction of temperatures.

1.4 Research Goals and Hypothesis

This study focuses on expanding to the body of quantitative analysis and applications of heat transport methods to further understand the influence of short term hydrologic events on the groundwater and surface water system by quantifying changes in magnitude and direction of flow within two Maine streambeds induced by storms and pumping of near stream groundwater wells. Average velocity values are calculated before, during, and after these short-term events in order to see how the flow is changing. The variance within each streambed is also analyzed. We hypothesize that (a) pumping tests will produce higher infiltration rates within the streambed at both locations and (b) there will be an increase in downward flow within the two streambeds throughout the duration of storm runoff events that result in elevated stream flow stage.

CHAPTER 2: SITE DESCRIPTIONS

In this study, data was collected from B Stream, a tributary of the Meduxnekeag River in northeastern Maine, and from the Stillwater River, a portion of the Penobscot River watershed in central Maine. The B Stream watershed has an area of 116 km^2 and drains into the Meduxnekeag River on the west side of Houlton, Maine. The land is covered predominantly by forests (79%) with about 17% of the area used for agriculture (Southern Aroostook County Soil and Water Conservation District, 1993). Bedrock of the B Stream watershed consists of steeply dipping calcareous and noncalcareous siltstones and calcic and dolomitic limestones that have been weakly metamorphosed (Pavilides, 1971). Surficial geology in the region is dominantly glacial till with scattered swamp deposits (Brewer, 1981). The Stillwater River is located on the west side of Marsh Island, breaking from the Penobscot River and flowing around the island and eventually rejoining the Penobscot at the south end of the island. The Penobscot River Watershed has an area of $21,476 \text{ km}^2$ and drains into the gulf of Maine (Dudley and Giffen, 2001). Bedrock below the Stillwater River consists of thick interbedded phyllite and metasiltstone (Griffen, 1976). Surficial geology is glacial till and glaciomarine deposits with an esker running along the river right banks of the Stillwater River (Maine Geological Survey, 2003). There is a deposit of wood waste, consisting of bark and wood chunks set in a matrix of sawdust with silt lining the bottom of the river (Emery and Garrett, 2002).

In rural areas, such as northern Maine, the use of groundwater as a source for drinking water is higher due to the high proportion of the population who source their water from private wells (Prescott, 1963). Groundwater resources in northern Maine are also under high demand for agricultural irrigation. Farmers concerned with potato quality

and reducing crop loss often increase groundwater usage to combat these concerns (Damicis and Baker, 2003). Water use in Aroostook County has increased 400% from 1982 to 1997, and the need for water continues to expand. The increased demand for water resource in Maine has prompted concern over the potential impact on the ecological health of surface-water systems. To address this concern, Maine has implemented low flow regulations (Maine Department of Environmental Protection, 2007), that restrict extraction of water that directly or indirectly reduces in-stream flow below a minimum amount considered necessary for ecosystem health.

Crocket station, the site of interest within the Meduxnekeag River Watershed for this study (Figure 1), is a retired water works building owned by the town of Houlton. This site was chosen due to its location on the banks of B Stream, and accessibility to the site (including land owner permission). Two 15 *cm* diameter bedrock wells (Crocket Well and Railroad Well) were installed in 2011 on the Crocket Station property measuring 30 *m* and 45 *m* deep and located 10 *m* and 30 *m* away from B Stream, respectively. Both wells are similar in construction to the majority of domestic wells located in Houlton, Maine with an open hole within the bedrock and a black steel casing through the unconsolidated material (fill and till) and about a foot into the bedrock. The Maine Geological Survey has 93 registered domestic wells in the town of Houlton, the majority of which (92 out of 93) are bedrock wells. Depths of these wells range from 7 *m* to 115 *m* (mean=57 *m*, 1 standard deviation=19 *m*). The Stillwater River site was chosen because Old Town water supply wells are located on the banks of the Stillwater, providing a setting where high pumping rates occur near a river (Figure 2). These surficial wells measure 15.4 *m* and 14 *m* deep with 60 *cm* diameter casings and are

located 30 *m* and 46 *m* from the Stillwater River (Emery and Garrett, 2002). These two locations allow us to compare how differing types of near stream groundwater extraction and geology influence the flow of water within the streambed.

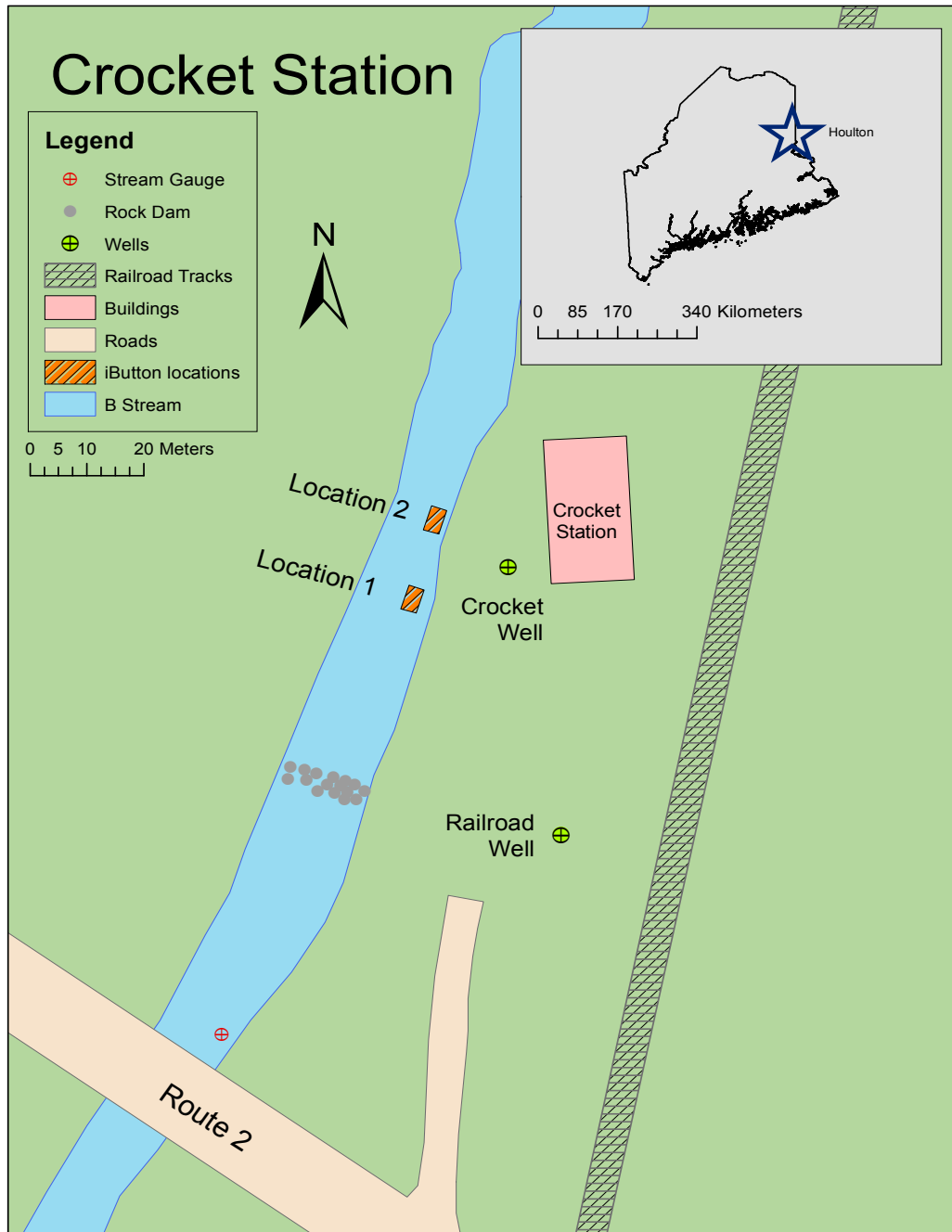


Figure 1: Map of the B Stream Field Site. The sample site is located in Houlton, Maine. The locations where iButtons were deployed in the stream are in orange and the green circles represent wells used for pumping tests.

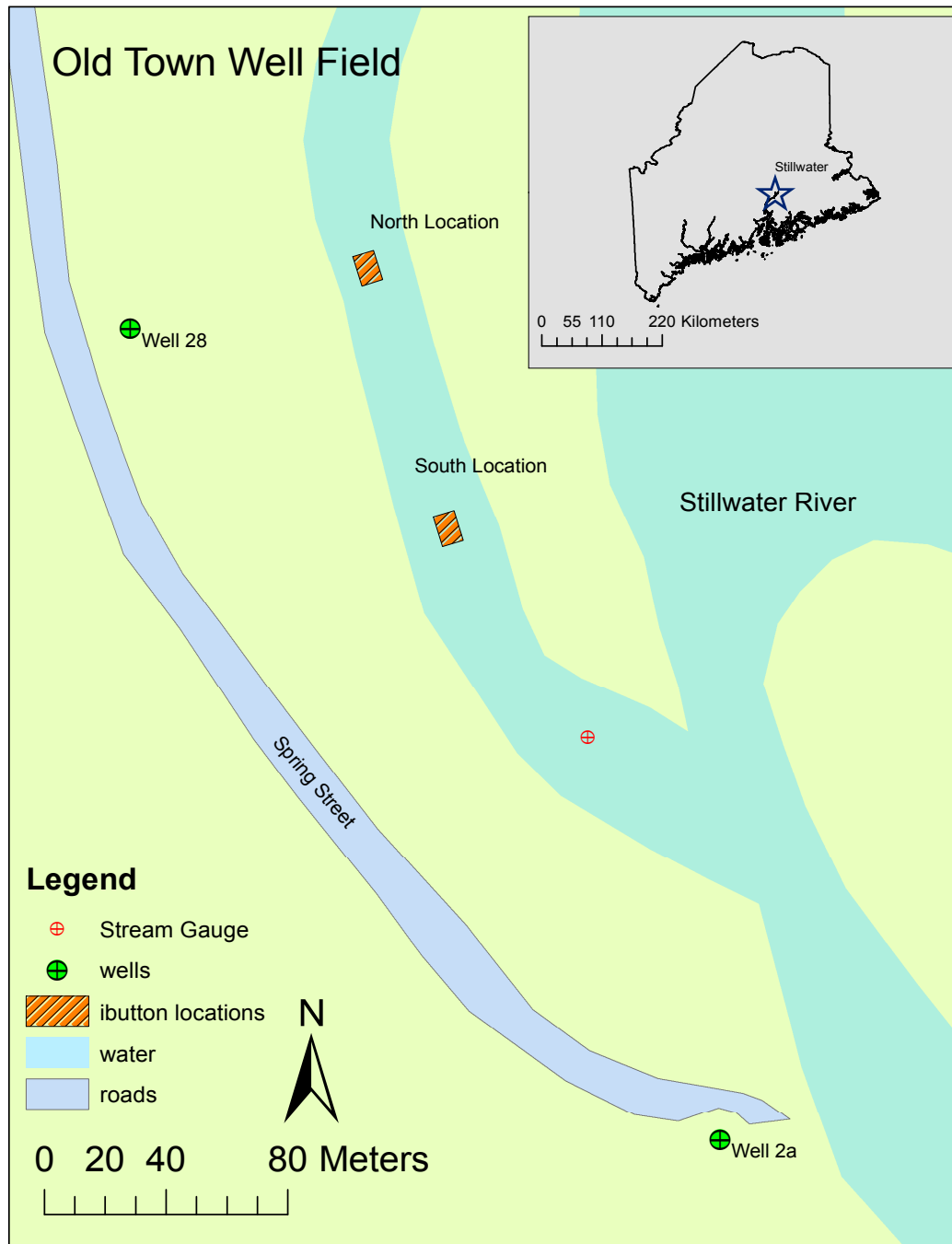


Figure 2: Map of the Stillwater River Site. The sample site is located in Old Town, Maine. The locations where iButtons were deployed in the stream are in orange and the green circles represent wells used for pumping tests.

CHAPTER 3: METHODS

3.1 Temperature Time Series Data

The flow of water within the streambed at both study sites was calculated by using streambed temperature time series to calibrate a numerical one-dimensional finite difference heat transport model. Temperature profiles were collected over 2 week periods during the summer of 2014 starting in early May and ending in early September. Temperature measurements were recorded with Thermochron iButtons (Dallas Semiconductor, Dallas Texas) models DS1922L and DS1921Z with accuracy of 0.5°C and 1.0°C and precision of $.125^{\circ}\text{C}$ and $.0625^{\circ}\text{C}$, respectively. The iButtons were programmed to record data at 10-minute intervals for 2 week periods. Each vertical profile was collected by placing four iButtons into a machined plastic rod with slots at intervals of 8 cm to assure consistent spacing of the iButtons (Figure 3). The slots housing the iButtons were sealed by covering the openings with electrical tape to waterproof the iButtons.



Figure 3: iButton and Deployment Stick. iButtons housed in the machined plastic rod. A U.S. quarter (2.42 cm diameter) is shown for scale.

iButton temperature loggers were deployed in two locations at each study site to assess the spatial and temporal variability of the flow of water within each streambed location. During each two-week collection period, two sets of six logger arrays were installed in a 2 by 3 rectangular configuration with spacing of 25 *cm* between each iButton rod (Figure 4). One array was placed in the streambed closest to the Crocket Well and the other was placed 3 *m* down stream from the first location. Each logger rod was pushed into the streambed until the top iButton was resting at the top of the streambed and the other three iButtons were at streambed depths of 8 *cm*, 16 *cm*, and 24 *cm*. Temperature profiles were collected from the Stillwater River four times during the summer of 2014 beginning on July 1st and ending on September 2nd. Two sets of four logger arrays were installed by a 2 X 2 configuration with spacing of 25 *cm* between each rod.

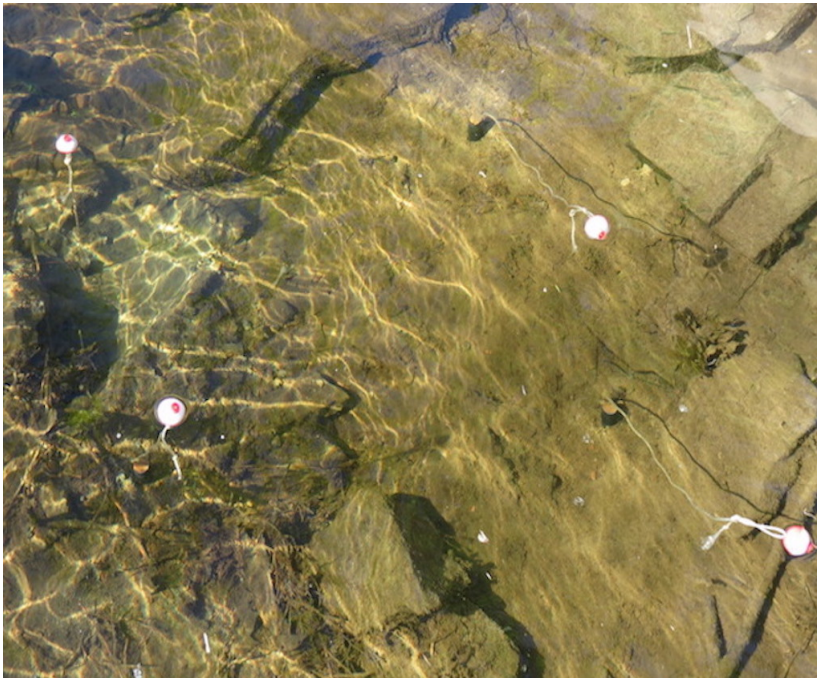


Figure 4: iButtons Deployed at the B Stream Site. This picture shows the temperature arrays deployed in the streambed of B Stream. Bobbers and string were attached to the top of the plastic rods for easy location. The spacing between each stick is 25cm.

3.2 Pumping Tests

Four separate pumping tests were executed on Crocket Station's two bedrock wells with the purpose of seeing how nearby groundwater extraction influenced the flow of water within the B Stream streambed. A 12volt DC Proactive™ Tornado 85 pump powered by two 12v 35AH AGM Deep Cycle batteries was used to Conduct two pumping tests on each well, one during high streamflow in the spring and one during low streamflow in the end of summer. There was a minimum duration of 10 days between each pumping test to allow for the system to recover. Each pumping test had duration of 3 hours with a pumping rate of 2 *l/min* to 3.5 *l/min* and was conducted during a two-week temperature collection period. Each pumping test resulted in the removal of about 720 *l* of groundwater, an amount of water that is greater than the average daily household use of 554 *l/day* (Hutson, 2004). A higher than average pumping rate was used for two reasons: 1) To avoid underestimation of the pumping effect on SBF and 2) to stress the system to accommodate the short time period of pumping provided by the batteries. Head changes in both wells were measured manually with electric water level tapes and an unvented pressure transducer (Solinst LeveLogger). Time series hydraulic pressure head data was collected from the well at intervals of 1 minute during the pumping tests and was corrected for atmospheric pressure changes by barometric pressure data retrieved from the Houlton International Airport (4.3 miles from Crocket Station). Drawdown data was analyzed using the Log-Log curve matching Theis method presented by Fitts (2013) to determine transmissivity of the two wells (Theis, 1935). Individual pumping tests were not completed on the Old Town wells. However, flow rates from the Old Town wells were provided by the Old Town water district. Stream stage data was collected using an

unvented pressure transducer (Solinst LeveLogger) placed in a stilling well that was attached to a metal rod driven into the river.

3.3 One-Dimensional Finite Difference Heat Transport Model

The direction and magnitude of the vertical groundwater flow within the streambed was calculated by calibrating a numerical one-dimensional finite difference model with the vertical temperature profiles collected during the summer of 2014. The model solves equation 1, the enthalpy dependent derivation of the heat transport equation used in the USGS model HST3D (Kipp, 1987). The model was created in a Python (van Rossum and Drake, 2011) script, using the Numpy (Oliphant, 2007) and Matplotlib (Hunter, 2007) libraries that enhance the numerical and plotting capabilities of the Python scripting language. The partial derivatives within equation 1 were approximated with finite difference methods (Slingerland and Kump, 2012). The conduction/dispersion term and the advection term are solved separately by using operator splitting. First, the conduction/dispersion term is solved using an implicit forward finite difference method (Slingerland and Kump, 2011). Second, an upwind scheme is used to solve the advective portion of the numerical model (Slingerland and Kump, 2011). The advective portion of equation 1 represents the water flux in and out of the cell and assumes all flow is vertical. The approximation for the partial derivative in the advective portion of equation 1 is dependent on the direction of groundwater flow. The approximation for the partial derivative within the advective term of equation 1 is given as

$$\frac{\partial T}{\partial x} = \frac{T_{front} - T_{back}}{\Delta x} \quad (5)$$

where T_{front} and T_{back} are the temperatures of the cells upstream of the respective cell face. This approximation can introduce instability within the model and is invalid when the stability criterion (eq 6) is violated (Slingerland and Kump, 2011). This method can also create numerical dispersion, especially where temperatures change rapidly over short distances (Slingerland and Kump, 2011).

$$\frac{|v| \cdot dt}{dx} < 1 \quad (6)$$

The stability of the upwind scheme (eq. 6) requires the product of the velocity (v) and the time step (dt) to be smaller than the size of the distance step (dx).

The one-dimensional vertical model has a total length of 5 m that is uniformly divided into 250 cells. Temperature is calculated in each of the 2 cm long cells over time to simulate the temporal temperature signal at different depths beneath the streambed. Temperatures are fixed at the top problem domain at each time step using measured streambed temperatures. A constant average annual temperature (6°C) was assigned to the bottom model cell. Thermal dispersion was assumed to be small and set to 0.005 $W/m \cdot C$. Values used for constant parameters can be found in table 1.

Model Property	B Stream	Stillwater	Units
Density of Fluid	1000	1000	$kg\ m^{-3}$
Density of solid	800	250	$kg\ m^{-3}$
Specific heat of fluid	4186	4186	$J\ kg^{-1}\ C^{-1}$
Specific heat of solid	1300	900	$J\ kg^{-1}\ C^{-1}$
Heat conduction of fluid	0.58	0.58	$W\ m^{-1}\ C^{-1}$
Heat conduction of solid	1.5	0.15	$W\ m^{-1}\ C^{-1}$
Porosity	0.2	0.7	-
Hydrodynamic Dispersion	0.005	0.005	$W\ m^{-1}\ C^{-1}$

Table 1: Model Parameter Values Used In Simulations

The direction and magnitude of the advective flux within the streambed, v *m/sec*, was estimated by minimizing the normalized squared residuals (R_{NSS}) between the measured and simulated temperatures at all three depths of 8 *cm*, 16 *cm*, and 24 *cm* (equation 7)

$$R_{NSS} = \frac{\sum_{i=1}^n (T_{i_meas} - T_{i_sim})^2}{n} \quad (7)$$

where T_{i_sim} and T_{i_meas} are the i^{th} value of the modeled and measured temperature time series data and n is the number of time steps. Running different velocity values ranging from -1×10^{-4} to 1×10^{-4} *m/s* through the model simulated the multiple temperature profiles used in calibration. The simulated profile with the lowest total combined R_{NSS} for all three depths was considered the best fit and the velocity parameter used to produce that modeled profile was assigned to the measured data. Negative and positive velocity values within the model indicate upward and downward flow, respectively, within the streambed. A velocity value of zero indicates a system with no vertical groundwater flow.

Temperature data was broken into 24 hour windows and the velocity was allowed to change at the beginning of each window in order to capture the potential transient response of changing advective flow over short periods (1 – 3 days) caused by the pumping tests and storms. Different vertical velocities are allowed in each time window and these velocities change as a step function in each time window (i.e. instantaneous change in velocity every 24 hours). The first day in each data set was considered a ‘warm-up’ period because the initial streambed temperatures are unknown and inaccurate

temperatures are impacted by the poorly constrained initial conditions (Lautz, 2010; Silliman et al., 1995).

Upward, downward, and no flow conditions were run through the model in order to see if it was responding to different flow conditions properly. Theoretically, the temperature signal at depth of a streambed with downward flow will have higher amplitude than that of a streambed with upward flow. The advective portion of equation 1 drives the propagation of the temperature signal into the streambed when the water is flowing down from the streambed and into the hyporheic zone. Figure 5 shows the simulated temperature curves, each with a different velocity values.

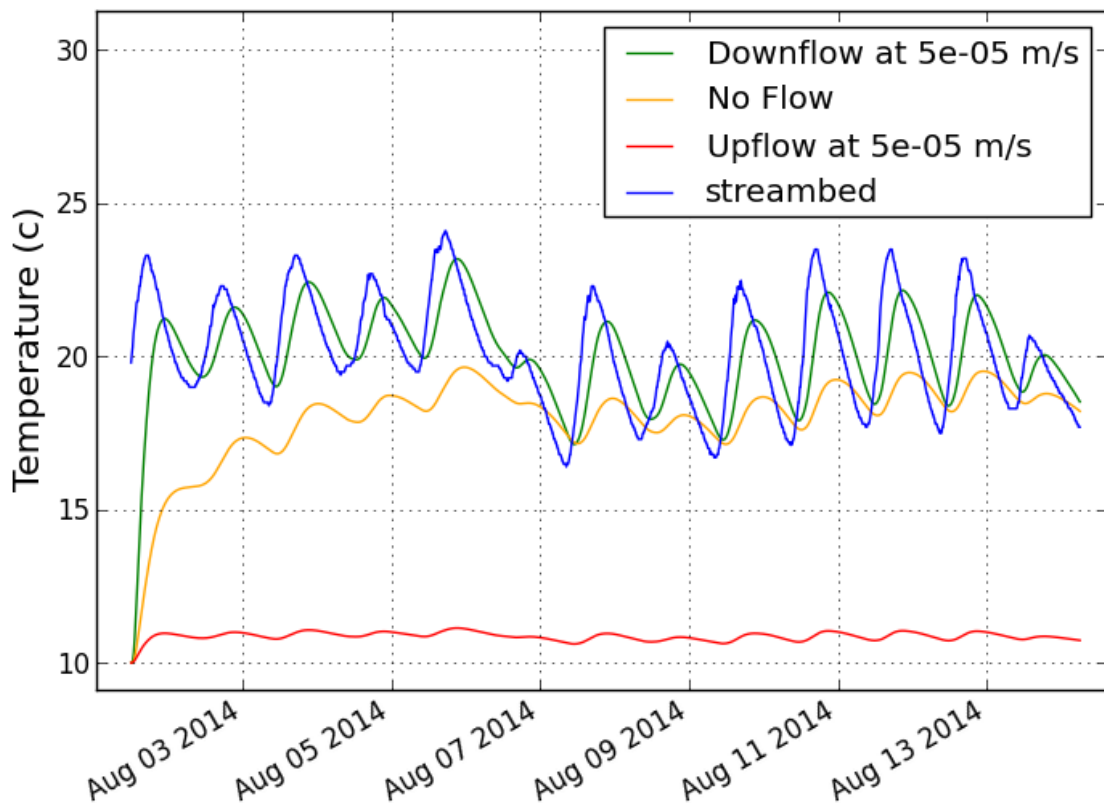


Figure 5: Varying Velocity Within the Model. Modeled temperature values at 14cm depth with upward (negative), downward (positive), and no flow conditions. The upflow condition (red curve) causes the advective portion of equation 1 to work against the propagation of the temperature signal, damping the amplitude of the signal.

CHAPTER 4: RESULTS

4.1 Pumping Tests

Pumping tests on the Crocket well (Figure 1) with pumping rates of 2 *l/min* and 3.5 *l/min* and durations of 3.5 hours for each test caused water level in wells to drop 302 *cm* and 1339 *cm*, respectively. Drawdowns of 4 *cm* and 10 *cm* were recorded in the Railroad well (Figure 1) during the pumping tests of the Crocket well. Transmissivity of the Crocket well was calculated to be 0.001 m^2/min . Pumping tests on the railroad well with pumping rates of 2 *l/min* and 3.5 *l/min* and durations of 3.5 hours caused water level in 324.2 *cm* and 712 *cm*, respectively. Drawdown of 6*cm* and 18 *cm* was recorded in the Crocket well during the pumping tests of the railroad well. Transmissivity of the railroad well was calculated to be 0.01 m^2/min .

4.2 Temperature Data

Streambed temperature data fluctuate diurnally within the streambed at both sites (Figure 6). Temperatures at depth are usually colder than those recorded at the surface. Amplitudes of the temperature signals at the B Stream location range from 3-4°C at the streambed to 0.5-1.0°C at depths of 24 *cm*, dampening with depth. Stillwater temperature signals exhibit a similar trend but have smaller amplitudes at the streambed (2-3°C) and at depth (no diurnal signal at 24 *cm* depth). Temperatures deviate away from sinusoidal patterns throughout the data and occur at both sites with durations of 1-3 days (Figure 7). Many deviations occur during or shortly after a precipitation event and/or a drop in air temperature.

Deviations occur as either a muting of the diurnal signal or as an inversion of the temperature gradient within the streambed (Figure 7). Temperature at the streambed drops quickly with the air temperature while the temperature at depth exhibits a

dampened and delayed response to the decreasing surface temperature, causing an inversion in the temperature profile. The decrease in temperature is followed by a recovery of the original temperature gradient and diurnal signal at or below temperatures recorded before the event.

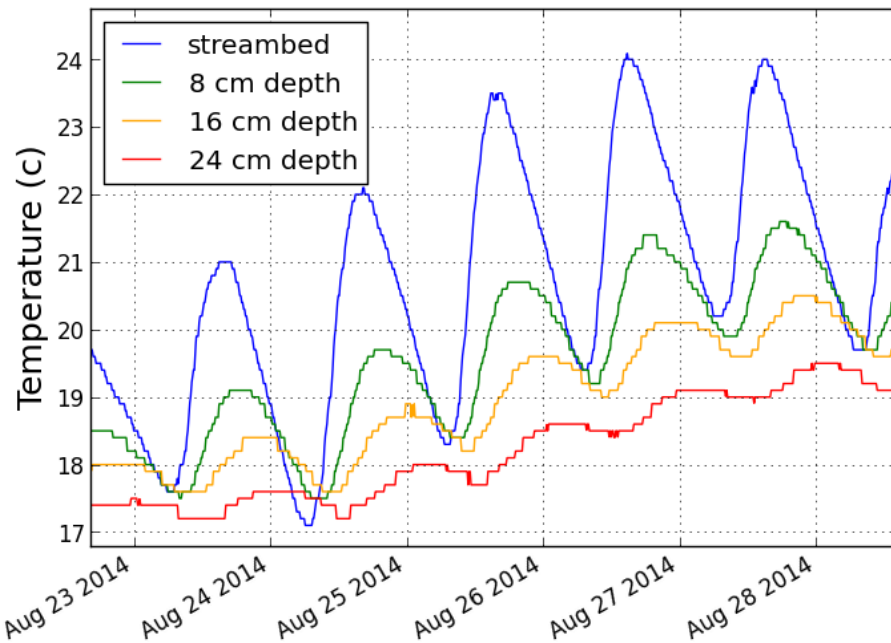


Figure 6: Measured Temperature Profile. Temperature data from one temperature array recorded at depth within the streambed of B Stream.

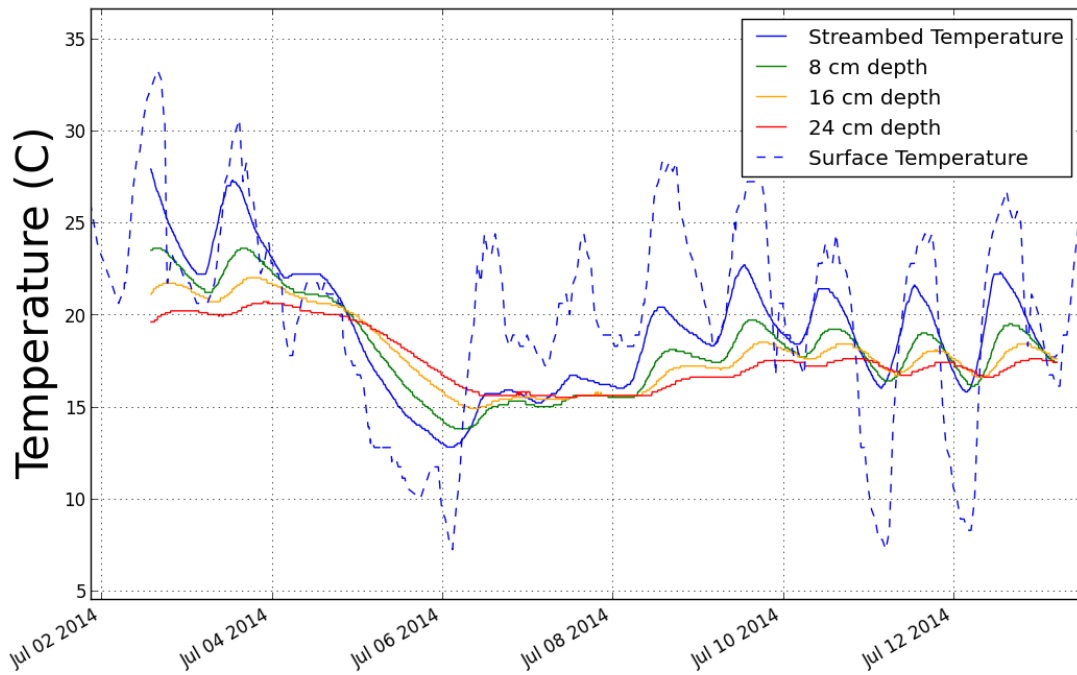


Figure 7: B Stream Temperatures During Hurricane Arthur. Hurricane Arthur moved through both field sites during the evening of July 4th to the afternoon of July 5th. An inversion is seen here from 5 July 2014, 00:00 to 6 July 2014 12:00. A muting of the temperature signal occurs after the inversion from 6 July 2014 12:00 to 7 July 2014 12:00.

4.3 Model Data

B Stream temperature data collected from June 3rd to July 13th and August 1st to September 12th were used to calibrate the heat transport model by adjusting the velocity parameter from equation 10. Two 14-day periods of data were not used as data from July 13th to July 31st was lost due to equipment error. Stillwater River temperature data collected from July 1st to July 15th and July 22nd to September 2nd were used for model calibration. Data collected from July 22nd to August 4th was lost due to equipment error. High water levels that prevented logger retrieval from July 15th to July 22nd caused the gap in the Stillwater River temperature data.

B Stream values extracted from daily model calibrations ranged from -5.27×10^{-5} m/sec to 2.74×10^{-5} m/s (mean = -1.13×10^{-5} m/s, standard deviation = 1.46×10^{-5} m/s) for

location 1 and from $-7.20 \times 10^{-5} \text{ m/s}$ to $3.80 \times 10^{-5} \text{ m/s}$ (mean = $-1.93 \times 10^{-5} \text{ m/s}$, standard deviation = $2.03 \times 10^{-5} \text{ m/s}$) for location 1. R_{NSS} of the daily windows ranged from 0.005°C to 0.209°C (mean = 0.028°C , standard deviation = 0.036°C). The majority of the daily extracted velocities at location 1 are upward, eight out of 55 are downward. The downward velocity values occur during three separate occasions from July 5th to July 7th, on August 14th, and from September 7th to September 12th (Figure 8). Location 2 exhibits similar trends with the majority of the daily extracted velocities being upward in flow direction and five days of downward velocity values occurring on July 5th and 6th, August 14th, and September 9th and 12th (Figure 9). Paired students t-tests (McClave and Sincich, 2009) indicate that there is a significant difference ($p=0.0004$) between the average extracted velocities from location 1 and 2.

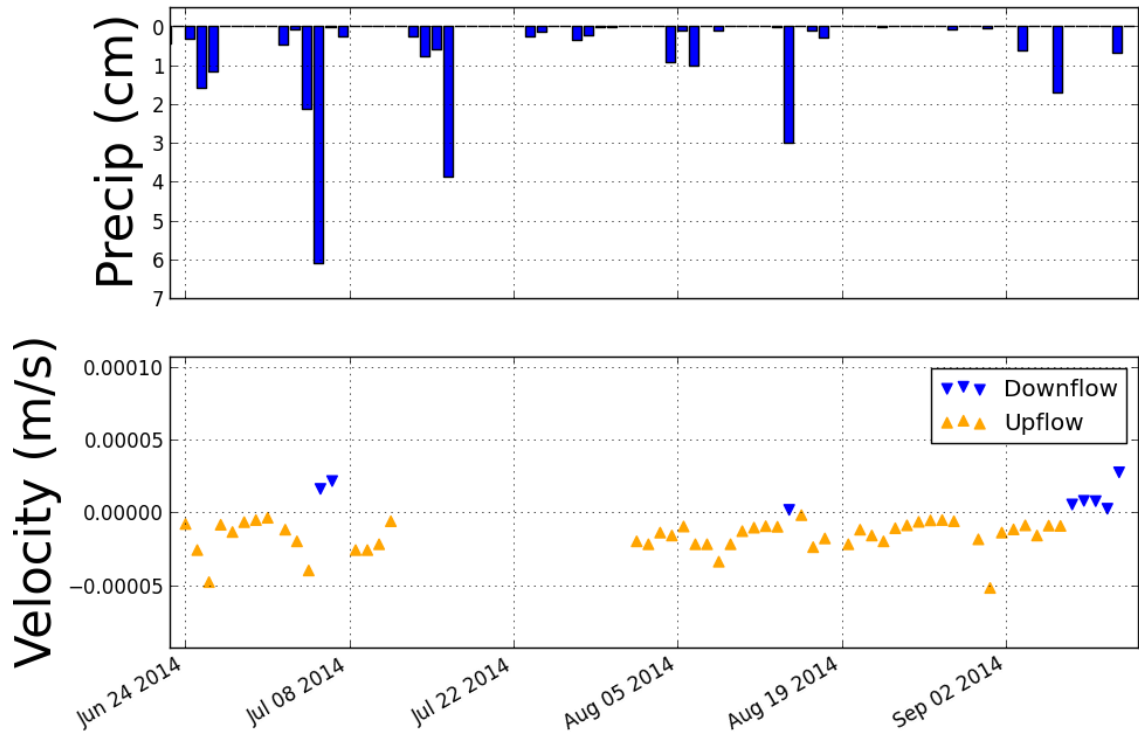


Figure 8: Average Velocities at Location 1 of the B Stream Site. Average velocities of location 1 in B Stream are plotted on the bottom portion of the plot. The top portion is the daily precipitation rates.

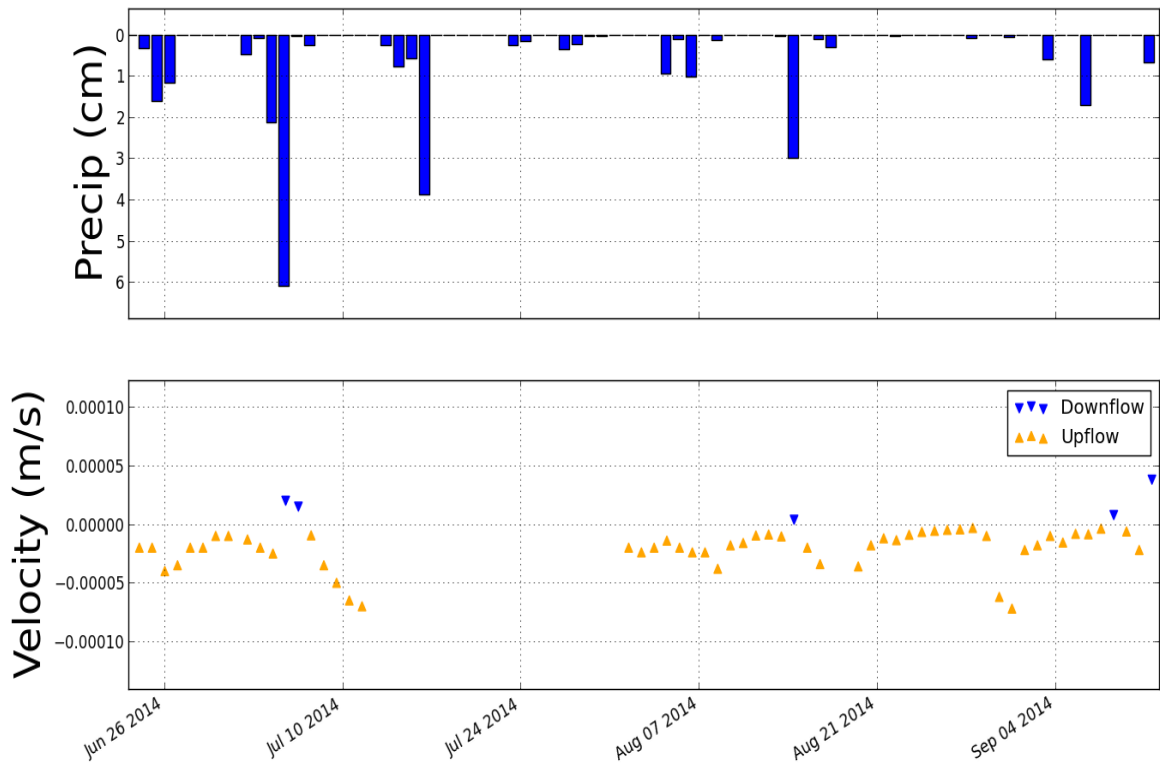


Figure 9: Average Velocities at Location 2 of the B Stream Site. Average velocities of location 2 in B Stream are plotted on the bottom portion of the plot. The top portion is the daily precipitation rates

Stillwater River velocity values extracted from daily model calibrations ranged from $-3.93 \times 10^{-5} \text{ m/s}$ to $-3.67 \times 10^{-7} \text{ m/s}$ (mean = $-4.38 \times 10^{-6} \text{ m/s}$, standard deviation = $8.02 \times 10^{-6} \text{ m/s}$) for the south location (Figure 10) and from $-7.67 \times 10^{-5} \text{ m/s}$ to $1.63 \times 10^{-6} \text{ m/s}$ (mean = $-5.01 \times 10^{-6} \text{ m/s}$, standard deviation = $1.34 \times 10^{-5} \text{ m/s}$) for the north location (Figure 11). R_{NSS} of the daily windows ranged from 0.005°C to 0.209°C (mean = 0.028°C , standard deviation = 0.036°C). The majority (46 out of 53) of the daily extracted velocities at the north location indicate upflow, seven out of 55 indicate downflow. The velocity values with downward flow occur once on August 20th and from August 22nd to August 28th the 25th and 28th. All of the daily extracted velocity values at the south

location are upward. A full account of all calculated velocities and errors can be found in tables 2.1 and 2.2. Paired students t-tests indicate that there is no significant difference ($p=0.624$) between the daily average velocities from the north and south locations before August 27th. However, paired students t-tests indicate there is a significant ($p=0.002$) difference between the daily average velocities from August 27th to September 2nd.

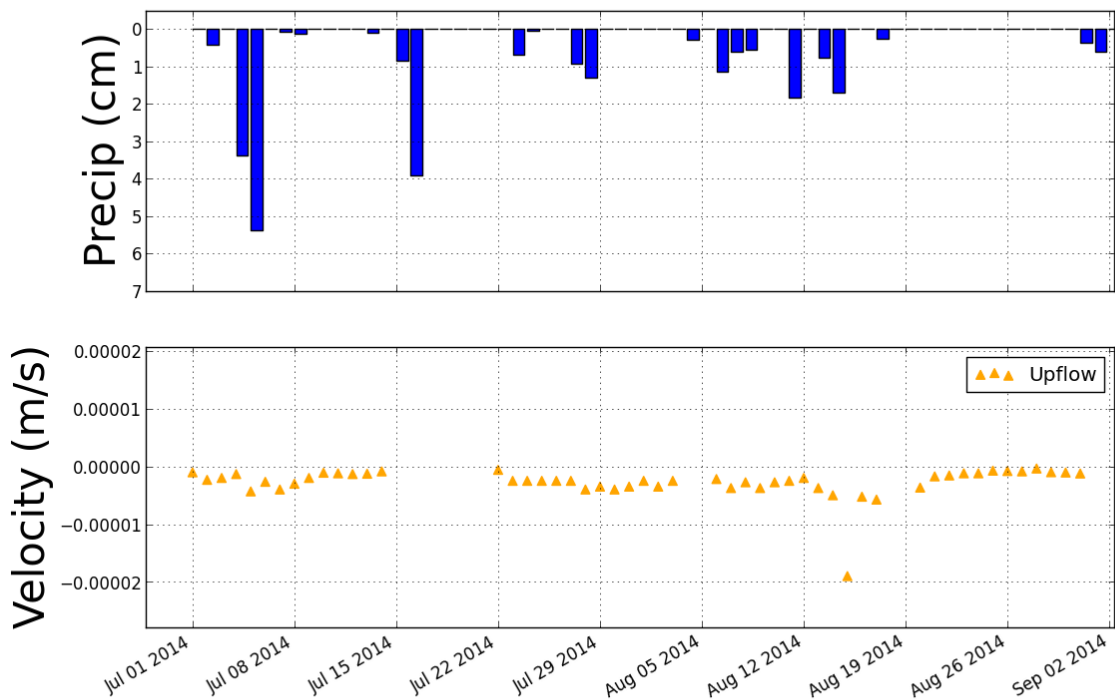


Figure 10: Average Velocities at the South Location of the Stillwater River Site. Average velocities of the south location in the Stillwater River are plotted on the bottom portion of the plot. The top portion is the daily precipitation rates

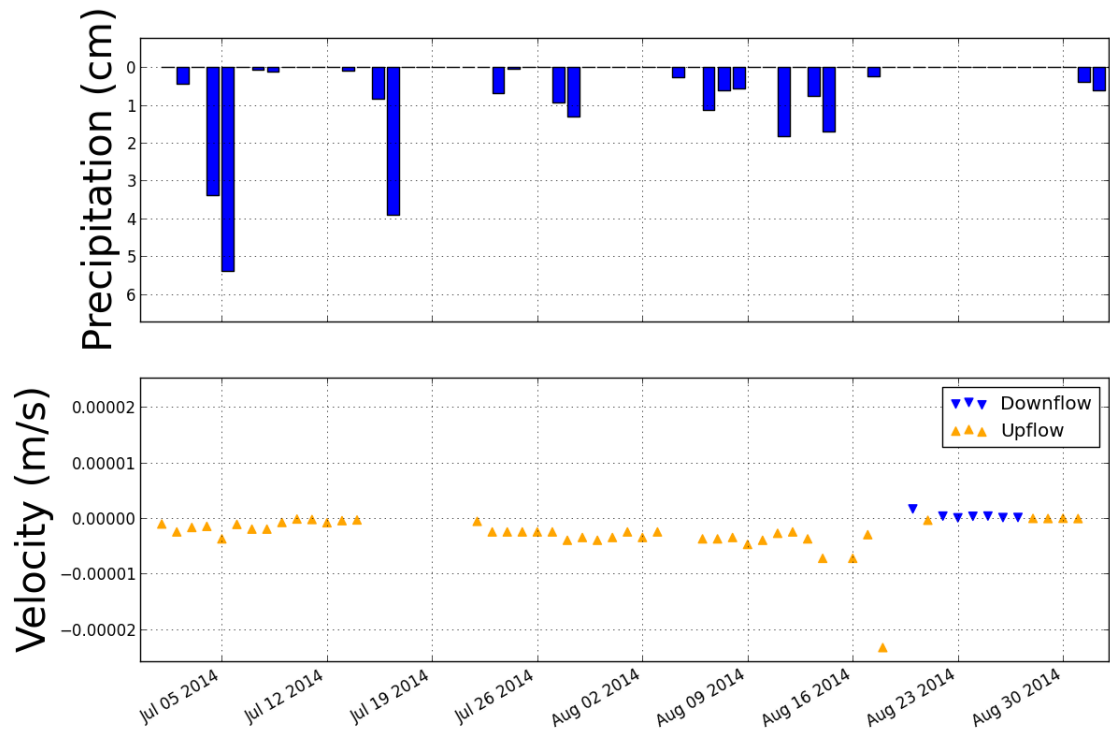


Figure 11: Average Velocities at the North Location of the Stillwater River Site. Average velocities of the north location in the Stillwater River are plotted on the bottom portion of the plot. The top portion is the daily precipitation rates

CHAPTER 5: DISCUSSION

5.1 Pumping Influence on Velocities

Daily model calibrations allowed for the analysis of the changes in groundwater flow within the streambed changed during short-term hydraulic events. Velocity outputs from the model indicate that the pumping tests conducted on the bedrock wells near B Stream had no effect on the direction of flow within the streambed (Figure 12). Reductions in hydraulic head were recorded in each well opposite of the well being pumped. This indicated that the cone of depression formed around the well being pumped had extended to the other well. Therefore it is known that the cone of depression forming around the pumped well had a radius no smaller than 45m. Both wells are closer than 45 *m* to the edge of the stream (6 *m* and 25 *m*) suggesting that the cone of depression extends to B Stream. The cone of depression should change the hydraulic gradient as it reaches the streambed. However, no significant change in the flow occurs within the model output. This result indicates that streamflow or hyporheic exchange within B Stream was not significantly impacted by the short term pumping tests. Additional testing necessary to determine if long term pumping would have impacted the groundwater velocity within the B Stream streambed.

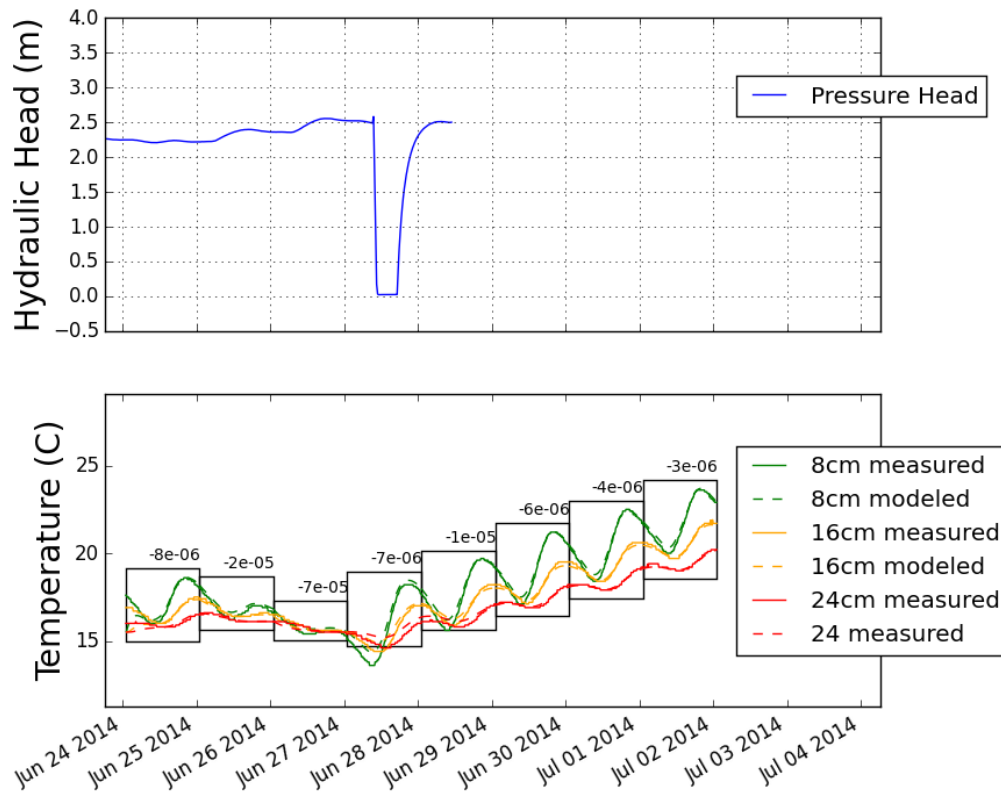


Figure 12: Average Velocities During June Pumping Test at B Stream. The top portion of Figure 8 shows the pressure head in the Crocket Well during the June pumping test. The bottom plot shows the measured and modeled temperature profiles recorded during the pumping test. The black boxes represent the windows of time that the model is calibrated to. The numbers above each window are the velocity values in *m/s* extracted for each individual window.

The surficial till unit that dominates the Houlton quadrangle (Brewer, 1981) could be decreasing the vertical effect of the expanding cone of depression and preventing it from influencing the SBF within B Stream. Glacial till in Maine has been shown to exhibit hydraulic conductivity values reaching as low as $3.5 \times 10^{-7} \text{ m/s}$ (Lyford et al., 1999). A low hydraulic conductivity till may reduce the hydraulic interconnection between the bedrock and the surficial unit, restricting flow of water from the surficial unit into the bedrock. If a low conductivity till were impeding the flow of water from the surficial unit into the bedrock, drawdown would occur in the bedrock with little impact to the surficial unit. Water would eventually begin to percolate into fractures from the surficial unit if the cone of depression was maintained for an extended period of time. However, hydraulic stress associated with short term pumping likely recovers before impacting the hydraulic gradients within the streambed. Higher pumping rates and extended pumping durations when compared to the tests executed in this study appear to be required for the pumping to have a significant effect on the flow of water within B Stream's streambed.

Velocity outputs from the model indicate that pumping of the surficial wells near the Stillwater River induced a shift in the direction of flow within the streambed (Figure 13). There was a shift in pumping rates on August 27th where well 28 was turned off and well 2a was turned on. The wells at the Stillwater River site are in surficial deposits and have very high pumping rates. The downward velocity values before the pump shut off indicate that well 28 is drawing water from the Stillwater river. Loggers from the north location recorded a shift from downward velocity values to upward velocity values on

August 28th. This shift in direction of flow is likely caused by the recovery of the cone of depression after well 28 was shut off.

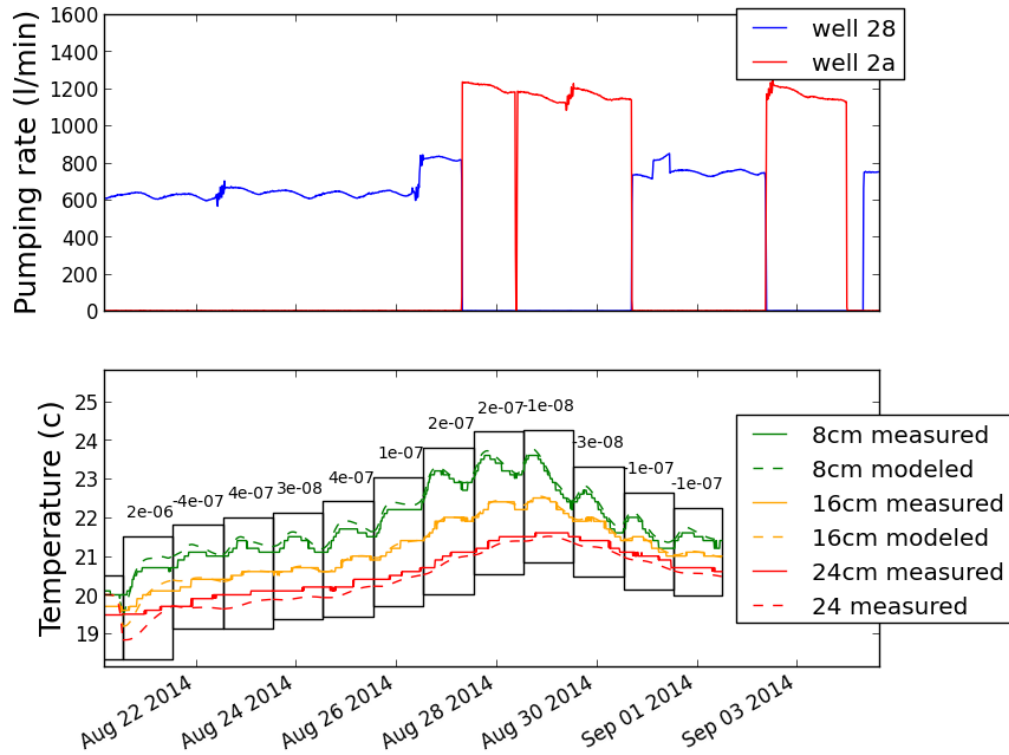


Figure 13: Average Velocities Pumping Rates at B Stream. Pumping rates from wells 28 and 2a vs. the modeled velocity values of the optimization windows at the Stillwater north location. Velocity values shift from upflow to downflow after well 28.

5.2 Storm Event Influence on Velocities

A mixture of upward and downward vertical groundwater velocities indicated by the calibrated simulations suggests that the direction of the groundwater flow in the streambed is shifting over time during storms in B Stream. Shifts in velocity at both B Stream sites are coincident with large rainfall events and increased stream water levels (Figures 8 and 9). The three periods with directional change of velocity occur within the model during and shortly (1-2 days) after the three largest (1.7 cm, 3 cm, and 8 cm of rain) precipitation events that occurred during data collection (Figure 14). The hydraulic gradient drives the flow of water (Freeze and Cherry, 1979) and higher water levels in B stream introduced by storms could lead to a change of the vertical hydraulic gradient. Boano et al. (2007) found that stream discharge and height fluctuations could cause variations in SBF. Hurricane Arthur, a weak tropical storm when it passed over Maine, had the highest rainfall rates and largest stream stage increase (1.5 m) measured during the study period. The output velocities from the model indicate a shift from upward to downward flow within the streambed during the increase in stream level (Figure 11). Flow then shifts back to upward flow after stream levels drop to previous storm levels. The two other large storms exhibit smaller but similar trends.

The Stillwater River model results do not exhibit the same directional change as seen in the B Stream results (Figure 15). Hurricane Arthur passed over the Stillwater River but the same directional shift in groundwater flow does not occur at either location. The velocity values at both Stillwater River locations exhibit upward flow and peak in magnitude during the elevated stream stage. Large watersheds have been shown to have muted or delayed responses in stage and discharge to precipitation events (Dingman, 2002). The stage of the Stillwater River peaked a day later than the stage of B Stream

after Hurricane Arthur. This delayed and muted response of stream stage could be limiting the effect of the storm on the SBF within the Stillwater River.

The differing geology between the Stillwater River and B Stream locations may be responsible for the differences in response of the velocity values. The esker located at the Stillwater site consists of medium sand to coarse gravel (Emery and Garrett, 2002). Typical hydraulic conductivity values of sand and gravel are magnitudes higher than typical hydraulic conductivity values of the fractured bedrock at the B Stream site. Water from precipitation events will most likely travel faster through the esker than the fractured bedrock. These differences in flow could be responsible for the differences in the direction of flow within the streambed observed between the two study sites.

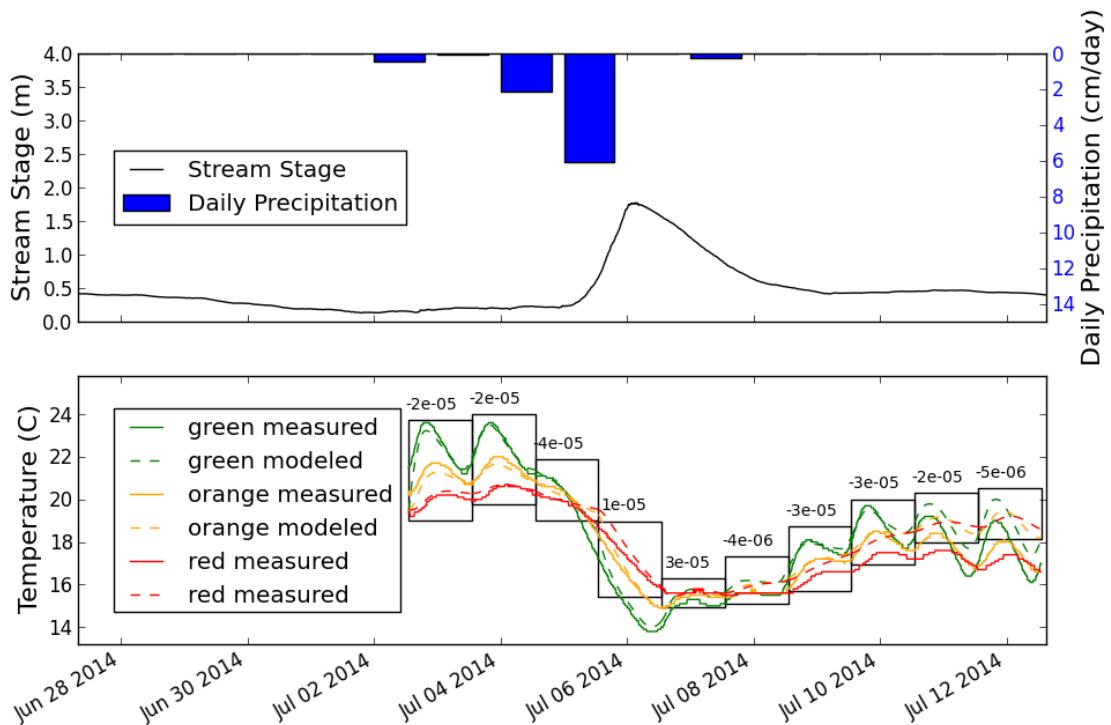


Figure 14: Average Velocities vs. Stream Stage and Precipitation at B Steam. Precipitation, stream stage, and modeled velocity value plots from top to bottom. The large increase in the stream stage could alter the hydraulic gradient within the streambed.

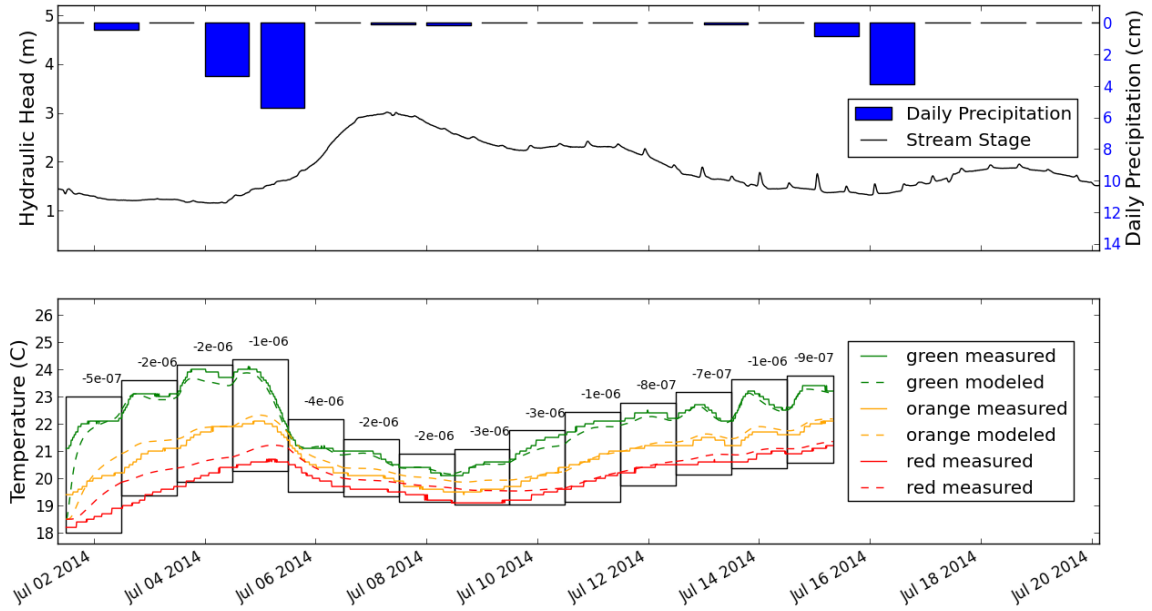


Figure 15: Average Velocities vs. Stream Stage and Precipitation at the Stillwater River. Precipitation and stream stage vs. the velocity values from a temperature array at the North Stillwater Location. No change in the sign of the velocity values occur, indicating no shift in direction of flow within the streambed.

These flow reversals have the potential to alter stream characteristics such as streambed chemistry (Zimmer and Lautz, 2014) and the ability of the stream to support habitat for fish (Brabrand et al., 2002). Zimmer and Lautz (2014) found that a rise in stream stage causes locations within the streambed that are surface water rich to be inundated with dilute event water. The change from upflow to downflow in B Stream recorded during Arthur will introduce surface water into an otherwise groundwater dominated portion of the streambed and has the potential to alter the chemistry within it. Changes in the residence time of water in the streambed caused by changes in flow have the potential to alter biogeochemical processes occurring in the streambed (Gooseff et al., (2003). Process such as the mineralization of dissolved organic carbon and nitrogen occur over periods of days to weeks and a change in flow had the potential to alter these

processes (Gooseff et al. 2003). Groundwater influx can control the amount of available habitat suitable for *salmonid* reproduction. Brabrand et al. (2002) found a correlation between *salmonid* redd density and the degree of groundwater influx. He attributed this result to the stable temperature regime provided by an influx of groundwater. Further research should investigate how these short-term reversals impact the quality of water and fish habitat within a stream.

The shift in direction of flow measured in the B Stream data is not a data artifact produced by the streambed temperature deviations brought by precipitation events. SBF shifts do not occur during all temperature deviations and are not associated with small precipitation events. For example, the streambed temperature drop of 28°C to 8°C from July 10th to July 11th (Figure 7) is not associated with a precipitation event and caused a small inversion of the temperature signal very similar to the inversion following the September 6th storm. However, unlike the velocity values following the September 6th storm, values stay upward throughout the inversion. Smaller ($>1.5\text{ cm}$) precipitation events do not have a significant effect on the flow of groundwater within the streambed. Rain events on August 6th and September 3rd had rainfall totals of $>1.5\text{ cm}$ and displayed non-sinusoidal temperature deviations. These events did not raise the stage of B Stream or the Stillwater River and did not have a significant effect on the direction or velocity of the SBF.

5.3 Variance Between Temperatures and Velocities

There is a significant difference ($p=0.004$) between the average velocities between the iButton locations in B Stream as indicated by the paired student's t-test. Location 2 at the B Stream site has a higher upward average velocity ($-1.93 \times 10^{-05}\text{ m/sec}$) than location 1 ($-1.13 \times 10^{-05}\text{ m/sec}$). Temperatures recorded at depth at location 2 should

be colder than temperatures at location 1 because of the stronger upward velocity at location 2. The average temperature signal at each location indicates that the temperatures collected at location 2 are consistently colder than temperatures at location 1 (Figure 16). Temperatures collected at a depth of 24 *cm* are on average 1.14°C colder at location 2 when compared to location 1. The average velocities between the iButton locations in the Stillwater River are not significantly different before well 28 was turned off. However opposing directions of flow Temperatures at both locations are very similar and differ by an average of 0.33°C (smaller than the iButton accuracy of 0.50°C) at a depth of 24 *cm* (Figure 17). The wood pulp material that lines the entire streambed of the sample locations and the sorted esker landform (Emery and Garrett, 2002) likely drive the lack of hydraulic variability and resulting streambed velocities and temperatures. The significant variability within B Stream is caused by the heterogeneity of the streambed, which is mainly composed of poorly sorted clays and glacial till (Pavilides, 1971).

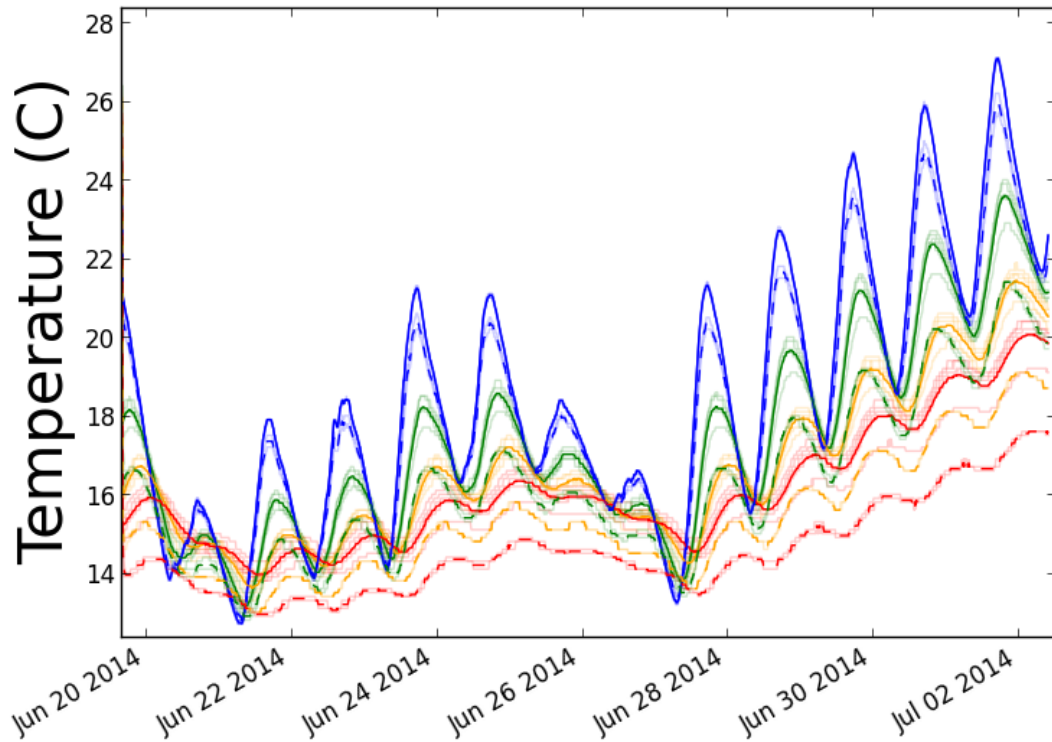


Figure 16: Average Temperatures at Both Locations of the B Stream Site. Average temperatures from B Stream at location 1 are plotted in the bold and full line. Average temperatures from B Stream at location 2 are plotted in the bold dashed line. All temperature measurements are plotted behind the bold lines. Blue lines are temperatures at the streambed and the green, orange, and red lines are temperatures at 8 cm, 16 cm, and 24 cm depth. Mean difference between the two sites was 0.37°C, 1.07°C, 1.31°C, and 1.54°C at depths of 0 cm, 8 cm, 16 cm, and 24 cm within the streambed.

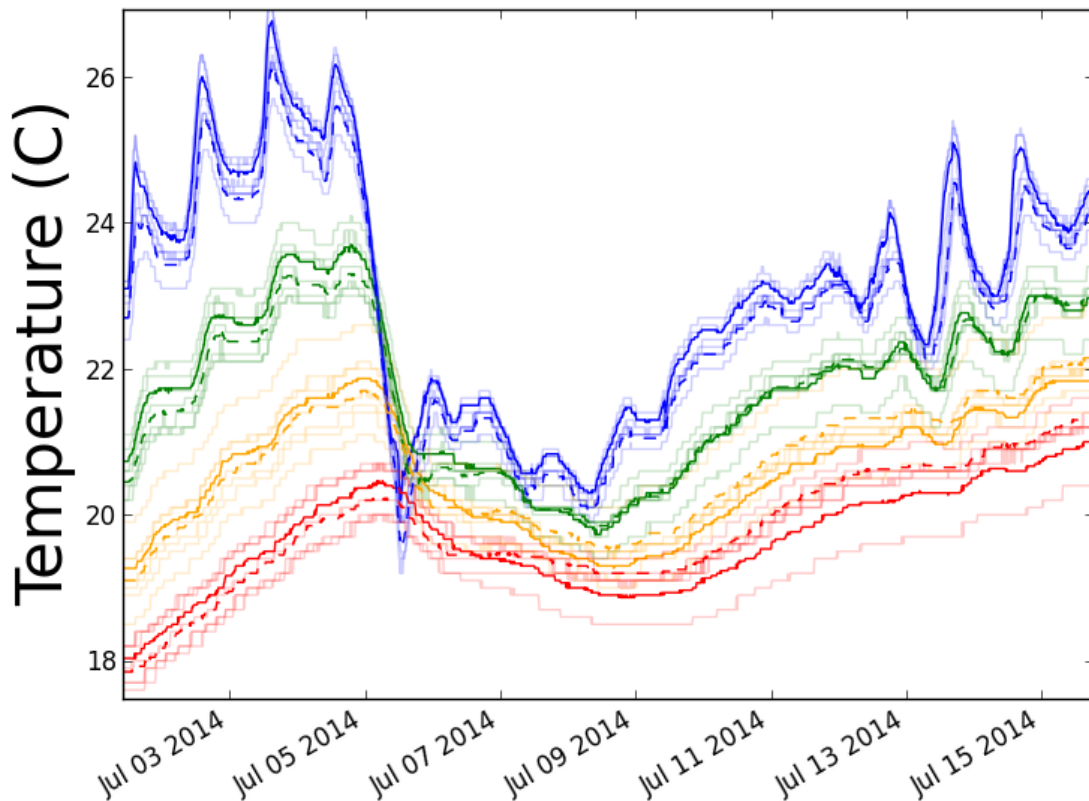


Figure 17: Average Temperatures at Both Locations of the Stillwater River Site. Average temperature at the south location is plotted in the bold and full line. Average temperature for the north location is plotted in the bold dashed line. All temperature measurements are plotted behind the bold lines. Blue lines are temperatures at the streambed and the green, orange, and red lines are temperatures at 8 cm, 16 cm, and 24 cm depths. Mean difference between the two sites was 0.35°C, 0.14°C, 0.22°C, and 0.27°C at depths of 0 cm, 8 cm, 16 cm, and 24 cm within the streambed.

CHAPTER 6: CONCLUSION

One-dimensional heat transport methods were used to assess the potential impact that near stream groundwater extraction and storms have on the flow of groundwater within the streambeds of B Stream (Houlton, Maine) and the Stillwater River (Old Town, Maine). Calibrations of a numerical one-dimensional heat transport model allow for the investigation of changes in transient groundwater flow within a streambed caused by short-term hydraulic events such as storms and nearby groundwater pumping. This analysis of temperature data collected in the Stillwater River confirm that flow within the streambed is affected by the pumping of large surficial aquifer wells located close to the stream. However, pumping smaller bedrock wells close to a stream in a location with low conductivity glacial till does not have an effect on the flow within the streambed. The analysis confirmed an increase in downward SBF directly after large (>1.5 cm) storm events at B Stream but not at the Stillwater River. Significant variance in average velocities between the two sample locations at B Stream was detected. This variance is likely to be a product of the streambed geology. Further study should focus on using short-term heat transport model calibration to investigate the potential impact of stream characteristics (geochemical, quality of fish habitat) caused by these short-term hydraulic events and how variance within the streambed alters the influence of pumping tests on the flow within the streambed.

REFERENCES

- Alley, WM, Reilly, TE and Franke, 1999. Sustainability of ground-water resources, U.S. Geological Survey Circular 1186.
- Anderson, M., 2005. Heat as a Ground Water Tracer, *Ground Water*, 43(6), 951–968, doi:10.1111/j.1745-6584.2005.00052.x.
- Anibas, C., Fleckenstein, J., Volze, N., Buis, K., Verhoeven, R., Meire, P. and Batelaan, O., 2009. Transient or steady-state? Using vertical temperature profiles to quantify groundwater-surface water exchange, *Hydrol. Pro Cess.*, 23 (15), 2165-2177, doi:10.1002/hyp.7289.
- Barlow, PM and Leake, 2012. *Streamflow Depletion by Wells: Understanding and Managing the Effects of Groundwater Pumping on Streamflow*, U.S. Geological Survey Circular 1376.
- Bear, J., 1988. *Dynamics of fluids in porous media*. New York: Dover.
- Brabrand, Å., Koestler, A. and Borgstrøm, R., 2002. Lake spawning of brown trout related to groundwater influx, *Journal of Fish Biology*, 60(3), 751–763, doi:10.1111/j.1095-8649.2002.tb01699.x.
- Bravo, H. R., Jiang, F., and Hunt, R. J., 2002. Using groundwater temperature data to constrain parameter estimation in a groundwater flow model of a groundwater flow model of a wetland system. *Water Resources Research*, 38(8), 1-14.
- Boano, F., Revelli, R. and Ridolfi, L., 2007. Bedform-induced hyporheic exchange with unsteady flows, *Advances in Water Resources*, 30(1), 148-156, doi:10.1016/j.advwatres.2006.03.004.
- Brewer, T., 1981. *Reconnaissance Surficial Geology of the Bridgewater, Houlton, Howe Brook, and Smyrna Mills Quadrangles, Maine*, Technical report, Maine Geological Survey.
- Briggs, M., Lautz, L., Hare, D. and González-Pinzón, R., 2013. Relating hyporheic fluxes, residence times, and redox-sensitive biogeochemical processes upstream of beaver dams, *Freshwater Science*, 33(2), doi:10.1899/12-110.1.
- Brunke, M., Gonser, T., 1997. The ecological significance of exchange processes between rivers and groundwater. *Freshwater Biol* 37, 1–3
- Calver, A., 2001. Riverbed Permeabilities: Information from Pooled Data, *Groundwater*, 39(4), 546–553, doi:10.1111/j.1745-6584.2001.tb02343.x.

- Conant, B., 2004. Delineating and Quantifying Ground Water Discharge Zones Using Streambed Temperatures, *Ground Water*, 42(2), 243–257, doi:10.1111/j.1745-6584.2004.tb02671.x.
- Constantz, J., 2008. Heat as a tracer to determine streambed water exchanges, *Water Resour. Res.*, 44(4), doi:10.1029/2008WR006996.
- Cuthbert, M. and Mackay, R., 2013. Impacts of nonuniform flow on estimates of vertical streambed flux, *Water Resour. Res.*, 49(1), 19–28, doi:10.1029/2011WR011587.
- Damicis, J and Baker, 2003. Aroostook County Economic Cluster Report Part 1: Analysis, [online] Available from: http://www.nmdc.org/pdf/Cluster_Report_Part_1.pdf.
- Dingman, S L., 2002. *Physical Hydrology*. Upper Saddle River, N.J: Prentice Hall.
- Dudley, RW and Giffen, SE, 2001. Composition and distribution of streambed sediments in the Penobscot River, Maine, U.S. Geological Survey Water-Resources Investigations Report 01-4223, May 1999.
- Dudley, RW and Stewart, GJ , 2007. Estimated Effects of Ground-Water Withdrawals on Streamwater Levels of the Pleasant River Near Crebo Flats, Maine, July 1 to September 30, 2005., U.S. Geological Survey Scientific Investigations Report 2006-5268.
- Ellis, P., Mackay, R. and Rivett, M., 2007. Quantifying urban river–aquifer fluid exchange processes: A multi-scale problem, *Journal of Contaminant Hydrology*, 91(1-2), 5880, doi:10.1016/j.jconhyd.2006.08.014.
- Ferguson, G. and Bense, V., 2011. Uncertainty in 1D Heat-Flow Analysis to Estimate Groundwater Discharge to a Stream, *Ground Water*, 49(3), 336–347, doi:10.1111/j.1745-6584.2010.00735.x.
- Fitts, C. R., 2013. *Groundwater Science*, Waltham, MA, Academic Press.
- Freeze, R.A., and Cherry, J.A., 1979. *Groundwater*: Englewood Cliffs, NJ, Prentice-Hall.
- Garrett, P., 2002. Technical Report: Hydrogeologic Investigations of Recharge to Spring Street Wellfield Stillwater, Old Town, Maine., Prepared for Old Town Water District, Old Town, Maine..
- Griffen, J.R., 1976. Reconnaissance Bedrock Geology of the Orono Quadrangle, Maine., Maine Geological Survey Open File 76-21.
- Gooseff, M., Wondzell, S., Haggerty, R., Anderson, J., 2003. Comparing transient storage modeling and residence time distribution (RTD) analysis in geomorphically

varied reaches in the Lookout Creek basin, Oregon, USA. *Advances in Water Resources* 26, 925937.

Goto, S., Yamano, M. and Kinoshita, M., 2005. Thermal response of sediment with vertical fluid flow to periodic temperature variation at the surface, *J. Geophys. Res.*, 110, B01106, doi:10.1029/2004JB003419.

Hatch, C., Fisher, A., Revenaugh, J., Constantz, J. and Ruehl, C., 2006. Quantifying surface water–groundwater interactions using time series analysis of streambed thermal records: Method development, *Water Resour. Res.*, 42(10), W10410, doi:10.1029/2005WR004787.

Healy, R.W., and Ronan, A.D., 1996, Documentation of computer program VS2DH for simulation of every transport in variably saturated porous media -- Modification of the U.S. Geological Survey's computer program VS2DT, *U.S. Geological Survey Water Resources Investigations Report* 90-4025, 125 p.

Heath, RC, 1983. Basic ground-water hydrology, U.S. Geological Survey, Water-Supply Paper 2220.

Hopmans, J., Šimunek, J. and Bristow, K., 2002. Indirect estimation of soil thermal properties and water flux using heat pulse probe measurements: Geometry and dispersion effects, *Water Resour. Res.*, 38(1), doi:10.1029/2000WR000071.

Hunter, J. D., 2007. Matplotlib: A 2D graphics environment, *Comput. Sci. Eng.*, 9(3), 90–95.

Hutson, SS, 2004. Estimated use of water in the United States in 2000, U.S. Geological Survey Circular 1268.

Ingebritsen, S. E. and Sanford, W. E., 1999. *Groundwater in geologic processes*, Cambridge University Press.

Kalbus, E., Reinstorf, F. and Schirmer, M., 2006. Measuring methods for groundwater – surface water interactions: a review, *Hydrol. Earth Syst. Sci.*, 10(6), 873–887, doi:10.5194/hess-10-873-2006.

Kalbus, E., Schmidt, C., Molson, J., Reinstorf, F. and Schirmer, M., 2009. Influence of aquifer and streambed heterogeneity on the distribution of groundwater discharge, *Hydrol. Earth Syst. Sci.*, 13(1), 69–77, doi:10.5194/hess-13-69-2009.

Keery, J., Binley, A., Crook, N. and Smith, J., 2007. Temporal and spatial variability of groundwater–surface water fluxes: Development and application of an analytical method using temperature time series, *Journal of Hydrology*, 336(1-2), 116, doi:10.1016/j.jhydrol.2006.12.003.

- Kipp, KL, 1987. HST3D; a computer code for simulation of heat and solute transport in three-dimensional ground-water flow systems, U.S. Geological Survey Water-Resources Investigations Report 86-4095.
- Krause, S., Bronstert, A. and Zehe, E., 2007. Groundwater–surface water interactions in a North German lowland floodplain – Implications for the river discharge dynamics and riparian water balance, *Journal of Hydrology*, 347(3-4), 404417, doi:10.1016/j.jhydrol.2007.09.028.
- LaBaugh, JW, Rosenberry, DO and Rosenberry, 2008. Field Techniques for Estimating Water Fluxes Between Surface Water and Ground Water, U.S. Geological Survey Techniques and Methods 4-D2.
- Lautz, L., 2010. Impacts of nonideal field conditions on vertical water velocity estimates from streambed temperature time series, *Water Resour. Res.*, 46, W01509, doi:10.1029/2009WR007917.
- Lyford, FP, Garabedian, SP and Hansen, BP, 1999. Estimated Hydraulic Properties for the Surficial-and Bedrock-Aquifer System, Meddybemps, Maine, U.S. Geological Survey Open-File Report 99-199.
- Malcolm, I., Soulsby, C., Youngson, A., Hannah, D., McLaren, I. and Thorne, A., 2004. Hydrological influences on hyporheic water quality: implications for salmon egg survival, *Hydro. Pro Cess.*, 18(9), 1543–1560, doi:10.1002/hyp.1405.
- Maine Department of Environmental Protection, 2007. 06-096 CMR Chapter 587, In-stream Flows and Lake and Pond Water Levels. <http://maine.gov/dep/water/rules/index.html>.
- Maine Geological Survey, 2003, Simplified surficial geologic map of Maine: Maine Geological Survey, 11' x 17' color map., scale 1:2,000,000.
- McClave, James T., and Terry Sincich, 2009. *Statistics*, Upper Saddle River, NJ: Pearson Prentice Hall.
- McDonald, MG and Harbaugh, AW, 1988. A modular three-dimensional finite-difference ground-water flow model, U.S. Geological Survey Techniques of Water-Resources Investigations, Book 6, Chapter A1.
- Oliphant, Travis E., 2007. *Python for Scientific Computing, Computing in Science & Engineering*, 9, 10-20, DOI:<http://dx.doi.org/10.1109/MCSE.2007.58>.
- Pavrides, L., 1971. Geologic map of the Houlton Quadrangle, Aroostook County, Maine., U.S. Geological Survey Map gq-920.
- Prescott, GC, 1963. Reconnaissance of ground-water conditions in Maine, U.S.

Geological Survey Water-Supply Paper 1669-T.

Rau GC; Andersen MS; McCallum AM; Roshan H; Acworth RI., 2014. Heat as a tracer to quantify water flow in near-surface sediments, *Earth-Science Reviews*, 129, 40-58, doi:10.1016/j.earscirev.2013.10.015.

Roshan, H., Rau, G., Andersen, M. and Acworth, I., 2012. Use of heat as a tracer to quantify vertical streambed flow in a two-dimensional flow field, *Water Resour. Res.*, 48 (10), doi:10.1029/2012WR011918.

Rugel, K., Jackson, C., Romeis, J., Golladay, S., Hicks, D. and Dowd, J., 2012. Effects of irrigation withdrawals on streamflows in a karst environment: lower Flint River Basin, Georgia, USA, *Hydrol. Pro Cess.*, 26(4), 523–534, doi:10.1002/hyp.8149.

Silliman, S., Ramirez, J. and McCabe, R., 1995. Quantifying downflow through creek sediments using temperature time series: one-dimensional solution incorporating measured surface temperature, *Journal of Hydrology*, 167(1-4), 99-119, doi:10.1016/0022-1694(94)02613-G.

Slingerland, Rudy., and Lee R. Kump., 2011. *Mathematical Modeling of Earth's Dynamical Systems: A Primer*. Princeton, N.J.: Princeton University Press.

Southern Aroostook County Soil and Water Conservation District, 1993. *Watershed protection plan/environmental assessment, main branch Meduxnekeag River watershed*, Aroostook County, Maine: Houlton, Maine, 86.

Stallman, R. W., 1965. Steady one-dimensional fluid flow in a semi-infinite porous medium with sinusoidal surface temperature, *J. Geophys. Res.*, 70(12), 2821–2827, doi: 10.1029/JZ070i012p02821.

Stonestrom, DA and Constantz, J, 2003. Heat as a tool for studying the movement of ground water near streams, *U.S. Geological Survey Circular 1260*.

Suzuki, S., 1960. Percolation measurements based on heat flow through soil with special reference to paddy fields, *Journal of Geophysical Research*, 65(9), 2883–2885, doi:10.1029/JZ065i009p02883.

Theis, C., 1935. The relation between the lowering of the piezometric surface and the rate and duration of discharge of a well using groune-water storage, *Trans. AGU*, 16(2), 519–524, doi:10.1029/TR016i002p00519.

van Rossum, G., and F. Drake, 2011. *The Python Language Reference Manual*, Network Theory Ltd., Godalming, United Kingdom.

Vandenbohede, A. and Lebbe, L., 2010. Parameter estimation based on vertical heat

transport in the surficial zone, *Hydrogeol J*, 18(4), 931–943, doi:10.1007/s10040-009-0557-5.

Westhoff, M., Bogaard, T. and Savenije, H., 2011. Quantifying spatial and temporal discharge dynamics of an event in a first order stream, using distributed temperature sensing, *Hydrol. Earth Syst. Sci.*, 15(6), 1945–1957, doi:10.5194/hess-15-1945-2011, 2011.

Zimmer, M. and Lautz, L., 2014. Temporal and spatial response of hyporheic zone geochemistry to a storm event, *Hydrol. Pro Cess.*, 28(4), 2324–2337, doi:10.1002/hyp.9778.

Zume, J. and Tarhule, A., 2007. Simulating the impacts of groundwater pumping on stream–aquifer dynamics in semiarid northwestern Oklahoma, USA, *Hydrogeol J*, 16(4), 797–810, doi:10.1007/s10040-007-0268-8.

APPENDIX A: PYTHON SCRIPTS

Heat Transport Model

```
def model_ss(V,file_list,start,stop,initial_guess):
    """
    Five arguments

    - 1st arg is the velocity of the flow
      (negative flow is up, positive flow is down) m/s
    - 2nd arg is the porosity of the material
    - 3rd arg is a list of 4 variables. Each variable is an output array from the read_data
      function. The order of the list should be blue, green, orange, red.
    - 4th arg is the start point (date) of optimization
    - 5th arg is the end point (date) for optimization

    - 4th and 5th argument should be in string format

    Ex: 'Jun 03 2014 12:00'

    Returns three objects

    - 1st is the error value
    - 2nd is the temperatures calculated at depth
    - 3rd is the dates of when the temperatures were calculated at

    """
    import numpy as np
    from read_data import read_data
    from copy import copy
    from dateutil.parser import parse
    # Heat term

    pf=1000. # density of fluid kg/m**3
    cf=4186. # specific heat of fluid joule/kg c
    ps=800 # density of solid kg/m**3
    cs=1300 # specific heat of solid joule/kg c
    n=.20
    Ke=(pf*cf*n+(1-n)*ps*cs)

    # Conduction and Dispersion
    kf=.58 # watts/m c
    ks=1.5 # watts/m c
    D=V*0.005
    Kcd=(n*kf+(1-n)*ks+n*D)

    # Advection
    Kv=n*pf*cf

    # Simplifying
    dt=3*60. # seconds in three minutes
    dx=.02 # meters
    C=(dt/dx**2)*(Kcd/Ke)

    # matrix
```

```

mtrx=np.zeros([250,250])
for i in range(250):
    for j in range(250):
        if (i==0) and (j==0):
            mtrx[i,j]=1
        elif (i==249) and (j==249):
            mtrx[i,j]=1
        elif (i==j):
            mtrx[i,j]=2*C+1
            mtrx[i,j-1]=-C
            mtrx[i,j+1]=-C

tsteps2=2
dt2=dt/tsteps2 # 3 minute steps (180 seconds) used in advection calculation

bed_temps=file_list[0]
green_temps=file_list[1]
orange_temps=file_list[2]
red_temps=file_list[3]

vect=initial_guess #18.5*np.ones([250]) # Initial Guess
vect[249]=10 # Setting the boundary condition
temp_at_depth=[]
if (V*dt2/dx)>1.:
    print 'stability violated'

number_of_rows=len(bed_temps)
for t in range(number_of_rows):
    vect[0]=bed_temps[t,1] # adding the streambed data to the vector
    solv=np.linalg.solve(mtrx,vect) # solving for conduction dispersion term
    temps=copy(solv)
    temps_old=copy(solv)

    for t2 in range(tsteps2): # solving for advective term
        if V>0:
            temps[1:-1]=(-Kv/Ke*V*dt2/dx)*(temps_old[1:-1]-temps_old[0:-
2])+temps_old[1:-1]
        else:
            temps[1:-1]=(-Kv/Ke*V*dt2/dx)*(temps_old[2:]-temps_old[1:-
1])+temps_old[1:-1]

    vect=copy(temps)
    temp_at_depth.append([temps[4],temps[8],temps[12]])

temp_at_depth=np.array(temp_at_depth)

# setting up optimization arrays
calculated_green=temp_at_depth[:,0]
measured_green=green_temps[:,1]

calculated_orange=temp_at_depth[:,1]
measured_orange=orange_temps[:,1]

```

```

calculated_red=temp_at_depth[:,2]
measured_red=red_temps[:,1]

dates=green_temps[:,0]

idx_start=np.where(dates==parse(start))
idx_stop=np.where(dates==parse(stop))

start=float(idx_start[0])
stop=float(idx_stop[0])

# Calculating error
diff_green=calculated_green[start:stop]-measured_green[start:stop]
diff_orange=calculated_orange[start:stop]-measured_orange[start:stop]
diff_red=calculated_red[start:stop]-measured_red[start:stop]
diff_green=np.absolute(diff_green)
diff_orange=np.absolute(diff_orange)
diff_red=np.absolute(diff_red)

aerr_green=np.sum(diff_green)/len(diff_green)
aerr_orange=np.sum(diff_orange)/len(diff_orange)
aerr_red=np.sum(diff_red)/len(diff_red)
ss=(aerr_green**0.5+aerr_orange**0.5+aerr_red**0.5)/3

return ss,temps,temp_at_depth,dates

```

Model optimization

```

import os
import numpy as np
import matplotlib.pyplot as plt
from dateutil.parser import parse
from read_data import read_data
from new_velocity_model import model_ss

# Setting up the optimization parameters

# path to data files
path=os.path.expanduser('~/.Desktop/thesis/data/corrected_data_houlton/houltonC_2014_09_12/')

# putting together velocity array
v5=np.array([[x*-1e-5 for x in range(9,0,-1)]])
v6=np.array([[x*-1e-6 for x in range(9,0,-1)]])
v7=np.array([[x*-1e-7 for x in range(9,0,-1)]])
v8=np.array([[x*-1e-8 for x in range(9,0,-1)]])
vp5=np.array([[x*1e-5 for x in range(9,0,-1)]])
vp6=np.array([[x*1e-6 for x in range(9,0,-1)]])
vp7=np.array([[x*1e-7 for x in range(9,0,-1)]])
vp8=np.array([[x*1e-8 for x in range(9,0,-1)]])
velocities=np.hstack((v5,v6,v7,v8,vp8,vp7,vp6,vp5))
length_v=np.shape(velocities)

```

```

velocities=np.reshape(velocities,(length_v[1],1))

dates=['Aug 29 2014 15:00','Aug 30 2014 15:00','Aug 31 2014 15:00','Sep 1 2014 15:00','Sep 2 2014
15:00',
'Sep 3 2014 15:00','Sep 4 2014 15:00','Sep 5 2014 15:00','Sep 6 2014 15:00','Sep 7 2014 15:00','Sep 8 2014
15:00',
'Sep 9 2014 15:00','Sep 10 2014 15:00','Sep 11 2014 15:00','Sep 12 2014 10:00']

f,(ax1,ax2,ax3,ax4,ax5,ax6,ax7,ax8,ax9,ax10) = plt.subplots(10, sharex=True)

#####

optimized_v001=[]
guess=18.5*np.ones([250]) # taking an initial guess at the temperature values
for i in range(len(dates)-1): # looping through each date window
    blue=read_data('001blue_h_2014_09_12shift.txt',path,dates[i],dates[i+1]) #reading in measured
    temperatures
    green=read_data('001green_h_2014_09_12shift.txt',path,dates[i],dates[i+1])
    orange=read_data('001orange_h_2014_09_12shift.txt',path,dates[i],dates[i+1])
    red=read_data('001red_h_2014_09_12shift.txt',path,dates[i],dates[i+1])
    file_list=[blue,green,orange,red]

    errors=[]

    for v in velocities: # calculate temperatures for each velocity values within the velocity array
        ss,temps,t_at_d,plotdates=model_ss(v,file_list,dates[i],dates[i+1],guess)
        errors.append([v,ss,t_at_d,temps])
        print '{0},{1},{2},{3}'.format(dates[i],dates[i+1],v,ss)

    errors=np.array(errors) # finding the minimum error
    err_col=errors[:,1]
    idx=err_col.argsort()[:2]
    fit=errors[idx]
    optimized_v001.append(fit)
    best=fit[0]
    best_temps=best[2]

    # setting the guess for the next window of data to the last column of temperatures in from the model run
    with the lowest error
    guess=best[3]

```

Read Data Script

```

def read_data(filename,path,start_date,end_date):
    """
    Four arguments
    - 1st arg is the name of the iButton file
    - 2nd arg is the path to file
    ex: path=os.path.expanduser('~/Desktop/maine/thesis/data/houlton_jun_19_2014/IButtons/')
    - 3rd arg is the start date and time of the data
    - 4th arg is the end date and time of the data

```

date time should be in the following format

'Jan 01 2014 13:00'

'''

```
from dateutil.parser import parse
import numpy as np
from dateutil import rrule
import time
import os

data=[]
flag=0
with open(path+filename,'r') as fl:
    for line in fl:
        line=line.decode(errors='ignore')
        words=line.split(',')
        if flag==1 and (len(words)>1):
            date=parse(words[0])
            temp=float(words[-1])
            data.append([date,temp])
        if ((words[0]=='TimeStamp')or(words[0]=='Date/Time')):
            flag=1

data=np.array(data)
idx=np.where((data[:,0]>parse(start_date))&(data[:,0]<parse(end_date)))
data=data[idx[0],:]

timevals=list(rrule.rrule(rrule.MINUTELY,dtstart=parse(start_date),
                           until=parse(end_date),interval=3))
timevals_epo Ch=np.array([time.mktime(a.timetuple()) for a in timevals])
data[:,0]=[time.mktime(a.timetuple()) for a in data[:,0]]
data=data.astype(np.float64)
data2=np.interp(timevals_epo Ch,data[:,0],data[:,1])

finaldata=np.vstack((np.array(timevals),data2))
return finaldata.transpose()
```

APPENDIX B: VELOCITY STATISTICS

Table 2: Stillwater Velocity Statistics at the North Location

Time Window	North Location				
	n=3 mean	median	max	min	R _{nss}
July/1/2014 12:00 to July/2/2014 12:00	-1.03E-06	-6.00E-07	-5.00E-07	-2.00E-06	0.456
July/2/2014 12:00 to July/3/2014 12:00	-2.33E-06	-2.00E-06	-2.00E-06	-3.00E-06	0.246
July/3/2014 12:00 to July/4/2014 12:00	-2.00E-06	-2.00E-06	-2.00E-06	-2.00E-06	0.195
July/4/2014 12:00 to July/5/2014 12:00	-1.33E-06	-1.00E-06	-1.00E-06	-2.00E-06	0.153
July/5/2014 12:00 to July/6/2014 12:00	-4.33E-06	-4.00E-06	-4.00E-06	-5.00E-06	0.095
July/6/2014 12:00 to July/7/2014 12:00	-2.67E-06	-2.00E-06	-2.00E-06	-4.00E-06	0.074
July/7/2014 12:00 to July/8/2014 12:00	-4.00E-06	-4.00E-06	-3.00E-06	-5.00E-06	0.075
July/8/2014 12:00 to July/9/2014 12:00	-3.00E-06	-3.00E-06	-2.00E-06	-4.00E-06	0.072
July/9/2014 12:00 to July/10/2014 12:00	-2.00E-06	-2.00E-06	-1.00E-06	-3.00E-06	0.084
July/10/2014 12:00 to July/11/2014 12:00	-1.10E-06	-8.00E-07	-5.00E-07	-2.00E-06	0.077
July/11/2014 12:00 to July/12/2014 12:00	-1.20E-06	-9.00E-07	-7.00E-07	-2.00E-06	0.065
July/12/2014 12:00 to July/13/2014 12:00	-1.33E-06	-1.00E-06	-1.00E-06	-2.00E-06	0.071
July/13/2014 12:00 to July/14/2014 12:00	-1.27E-06	-9.00E-07	-9.00E-07	-2.00E-06	0.082
July/14/2014 12:00 to July/15/2014 12:00	-8.67E-07	-8.00E-07	-8.00E-07	-1.00E-06	0.069
July/22/2014 12:00 to July/23/2014 12:00					
July/23/2014 12:00 to July/24/2014 12:00					
July/24/2014 12:00 to July/25/2014 12:00					
July/25/2014 12:00 to July/26/2014 12:00					
July/26/2014 12:00 to July/27/2014 12:00					
July/27/2014 12:00 to July/28/2014 12:00					

Table 2. Continued

No Data Collected Due to Equipment Error					
July/28/2014 12:00 to July/29/2014 12:00					
July/29/2014 12:00 to July/30/2014 12:00					
July/30/2014 12:00 to July/31/2014 12:00					
July/31/2014 12:00 to Aug/1/2014 12:00					
Aug/1/2014 12:00 to Aug/2/2014 12:00					
Aug/2/2014 12:00 to Aug/3/2014 12:00					
Aug/3/2014 12:00 to Aug/4/2014 12:00					
	n=4				
	mean	median	max	min	R _{nss}
Aug/6/2014 9:00 to Aug/7/2014 9:00	-3.75E-06	-3.50E-06	-2.00E-06	-6.00E-06	0.193
Aug/7/2014 9:00 to Aug/8/2014 9:00	-3.75E-06	-4.00E-06	-2.00E-06	-5.00E-06	0.223
Aug/8/2014 9:00 to Aug/9/2014 9:00	-3.50E-06	-3.50E-06	-3.00E-06	-4.00E-06	0.196
Aug/9/2014 9:00 to Aug/10/2014 9:00	-4.75E-06	-5.00E-06	-3.00E-06	-6.00E-06	0.188
Aug/10/2014 9:00 to Aug/11/2014 9:00	-4.00E-06	-4.00E-06	-3.00E-06	-5.00E-06	0.201
Aug/11/2014 9:00 to Aug/12/2014 9:00	-2.75E-06	-3.00E-06	-2.00E-06	-3.00E-06	0.189
Aug/12/2014 9:00 to Aug/13/2014 9:00	-2.50E-06	-2.50E-06	-2.00E-06	-3.00E-06	0.185
Aug/13/2014 9:00 to Aug/14/2014 9:00	-3.75E-06	-4.00E-06	-3.00E-06	-4.00E-06	0.155
Aug/14/2014 9:00 to Aug/15/2014 9:00	-7.25E-06	-7.50E-06	-5.00E-06	-9.00E-06	0.149
Aug/15/2014 9:00 to Aug/16/2014 9:00	-3.75E-05	-4.00E-05	-2.00E-05	-5.00E-05	0.164
Aug/16/2014 9:00 to Aug/17/2014 9:00	-7.25E-06	0.00E+00	1.00E-06	-3.00E-05	0.135
Aug/17/2014 9:00 to Aug/18/2014 9:00	-3.00E-06	-3.00E-06	-2.00E-06	-4.00E-06	0.104
	n=3				
	mean	median	max	min	R _{nss}
Aug/18/2014 13:00 to Aug/19/2014 13:00	-2.33E-05	-2.00E-05	-2.00E-05	-3.00E-05	0.224
Aug/19/2014 13:00 to Aug/20/2014 13:00	-7.67E-05	-8.00E-05	-7.00E-05	-8.00E-05	0.355
Aug/20/2014 13:00 to Aug/21/2014 13:00	1.63E-06	2.00E-06	2.00E-06	9.00E-07	0.271
Aug/21/2014 13:00 to Aug/22/2014 13:00	-4.00E-07	-4.00E-07	-2.00E-07	-6.00E-07	0.186
Aug/22/2014 13:00 to Aug/23/2014 13:00	3.40E-07	4.00E-07	7.00E-07	-8.00E-08	0.177

Table 2. Continued

Aug/23/2014 13:00 to Aug/24/2014 13:00	4.00E-08	3.00E-08	8.00E-08	1.00E-08	0.163
Aug/24/2014 13:00 to Aug/25/2014 13:00	3.13E-07	4.00E-07	5.00E-07	4.00E-08	0.167
Aug/25/2014 13:00 to Aug/26/2014 13:00	3.47E-07	1.00E-07	9.00E-07	4.00E-08	0.154
Aug/26/2014 13:00 to Aug/27/2014 13:00	8.33E-08	3.00E-08	2.00E-07	2.00E-08	0.133
Aug/27/2014 13:00 to Aug/28/2014 13:00	1.00E-07	2.00E-07	3.00E-07	-2.00E-07	0.152
Aug/28/2014 13:00 to Aug/29/2014 13:00	-7.00E-08	-1.00E-08	1.00E-07	-3.00E-07	0.136
Aug/29/2014 13:00 to Aug/30/2014 13:00	-9.00E-08	-1.00E-07	3.00E-08	-2.00E-07	0.160
Aug/30/2014 13:00 to Aug/31/2014 13:00	-5.00E-08	-9.00E-08	4.00E-08	-1.00E-07	0.156
Aug/31/2014 13:00 to Sep/1/2014 13:00	-1.00E-07	-1.00E-07	3.00E-07	-5.00E-07	0.124
Students T-Test (paired) Between Locations	p=.624				

Table 2: Mean, median, max, min, and R_{nss} of the Stillwater River velocity data from the north location.

Table 3. Continued

Table 3: Stillwater Velocity Statistics at the South Location

Time Window	South Location				
	n=4 mean	median	max	min	R _{nss}
July/1/2014 12:00 to July/2/2014 12:00	-1.08E-06	-1.45E-06	6.00E-07	-2.00E-06	0.459
July/2/2014 12:00 to July/3/2014 12:00	-2.50E-06	-2.50E-06	-2.00E-06	-3.00E-06	0.306
July/3/2014 12:00 to July/4/2014 12:00	-1.70E-06	-2.00E-06	-8.00E-07	-2.00E-06	0.237
July/4/2014 12:00 to July/5/2014 12:00	-1.50E-06	-1.50E-06	-1.00E-06	-2.00E-06	0.208
July/5/2014 12:00 to July/6/2014 12:00	-3.75E-06	-4.00E-06	-3.00E-06	-4.00E-06	0.144
July/6/2014 12:00 to July/7/2014 12:00	-1.15E-06	-1.00E-06	-6.00E-07	-2.00E-06	0.104
July/7/2014 12:00 to July/8/2014 12:00	-2.00E-06	-2.00E-06	-1.00E-06	-3.00E-06	0.110
July/8/2014 12:00 to July/9/2014 12:00	-2.00E-06	-2.00E-06	-1.00E-06	-3.00E-06	0.101
July/9/2014 12:00 to July/10/2014 12:00	-8.00E-07	-7.50E-07	-7.00E-07	-1.00E-06	0.116
July/10/2014 12:00 to July/11/2014 12:00	-1.83E-07	-1.95E-07	6.00E-08	-4.00E-07	0.107
July/11/2014 12:00 to July/12/2014 12:00	-2.70E-07	-2.50E-07	-8.00E-08	-5.00E-07	0.113
July/12/2014 12:00 to July/13/2014 12:00	-8.50E-07	-1.00E-06	-4.00E-07	-1.00E-06	0.103
July/13/2014 12:00 to July/14/2014 12:00	-4.75E-07	-4.50E-07	-2.00E-07	-8.00E-07	0.107
July/14/2014 12:00 to July/15/2014 12:00	-3.50E-07	-3.50E-07	-2.00E-07	-5.00E-07	0.106
	n=2 mean	median	max	min	R _{nss}
July/22/2014 12:00 to July/23/2014 12:00	-	-	0.0000008	-0.000002	0.330
July/23/2014 12:00 to July/24/2014 12:00	-2.50E-06	-2.50E-06	-2.00E-06	-3.00E-06	0.118
July/24/2014 12:00 to July/25/2014 12:00	-2.50E-06	-2.50E-06	-2.00E-06	-3.00E-06	0.079
July/25/2014 12:00 to July/26/2014 12:00	-2.50E-06	-2.50E-06	-2.00E-06	-3.00E-06	0.082
July/26/2014 12:00 to July/27/2014 12:00	-2.50E-06	-2.50E-06	-2.00E-06	-3.00E-06	0.073
July/27/2014 12:00 to July/28/2014 12:00	-2.50E-06	-2.50E-06	-2.00E-06	-3.00E-06	0.071
July/28/2014 12:00 to	-4.00E-06	-4.00E-06	-3.00E-06	-5.00E-06	0.098

Table 3. Continued

July/29/2014 12:00					
July/29/2014 12:00 to July/30/2014 12:00	-3.50E-06	-3.50E-06	-3.00E-06	-4.00E-06	0.088
July/30/2014 12:00 to July/31/2014 12:00	-4.00E-06	-4.00E-06	-4.00E-06	-4.00E-06	0.095
July/31/2014 12:00 to Aug/1/2014 12:00	-3.50E-06	-3.50E-06	-3.00E-06	-4.00E-06	0.098
Aug/1/2014 12:00 to Aug/2/2014 12:00	-2.50E-06	-2.50E-06	-2.00E-06	-3.00E-06	0.092
Aug/2/2014 12:00 to Aug/3/2014 12:00	-3.50E-06	-3.50E-06	-3.00E-06	-4.00E-06	0.092
Aug/3/2014 12:00 to Aug/4/2014 12:00	-2.50E-06	-2.50E-06	-2.00E-06	-3.00E-06	0.079
	n=4				
	mean	median	max	min	R _{nss}
Aug/6/2014 9:00 to Aug/7/2014 9:00	-2.19E-06	-2.35E-06	-7.00E-08	-4.00E-06	0.249
Aug/7/2014 9:00 to Aug/8/2014 9:00	-3.75E-06	-4.00E-06	-2.00E-06	-5.00E-06	0.150
Aug/8/2014 9:00 to Aug/9/2014 9:00	-2.75E-06	-2.50E-06	-2.00E-06	-4.00E-06	0.101
Aug/9/2014 9:00 to Aug/10/2014 9:00	-3.75E-06	-4.00E-06	-2.00E-06	-5.00E-06	0.107
Aug/10/2014 9:00 to Aug/11/2014 9:00	-2.75E-06	-2.50E-06	-2.00E-06	-4.00E-06	0.101
Aug/11/2014 9:00 to Aug/12/2014 9:00	-2.50E-06	-2.50E-06	-2.00E-06	-3.00E-06	0.102
Aug/12/2014 9:00 to Aug/13/2014 9:00	-2.00E-06	-2.00E-06	-2.00E-06	-2.00E-06	0.102
Aug/13/2014 9:00 to Aug/14/2014 9:00	-3.75E-06	-4.00E-06	-2.00E-06	-5.00E-06	0.097
Aug/14/2014 9:00 to Aug/15/2014 9:00	-5.00E-06	-5.00E-06	-3.00E-06	-7.00E-06	0.097
Aug/15/2014 9:00 to Aug/16/2014 9:00	-1.90E-05	-1.65E-05	-3.00E-06	-4.00E-05	0.106
Aug/16/2014 9:00 to Aug/17/2014 9:00	-5.25E-06	-4.00E-06	-3.00E-06	-1.00E-05	0.084
Aug/17/2014 9:00 to Aug/18/2014 9:00	-5.75E-06	-4.50E-06	-4.00E-06	-1.00E-05	0.101
	n=3				
	mean	median	max	min	R _{nss}
Aug/18/2014 13:00 to Aug/19/2014 13:00	-3.93E-05	-2.00E-05	-8.00E-06	-9.00E-05	0.308
Aug/19/2014 13:00 to Aug/20/2014 13:00	-3.33E-05	-2.00E-05	-1.00E-05	-7.00E-05	0.391
Aug/20/2014 13:00 to Aug/21/2014 13:00	-3.67E-06	-4.00E-06	-1.00E-06	-6.00E-06	0.177
Aug/21/2014 13:00 to Aug/22/2014 13:00	-1.73E-06	-1.00E-06	-2.00E-07	-4.00E-06	0.171
Aug/22/2014 13:00 to	-1.57E-06	-6.00E-07	-1.00E-07	-4.00E-06	0.189

Table 3. Continued

Aug/23/2014 13:00					
Aug/23/2014 13:00 to					
Aug/24/2014 13:00	-1.20E-06	-4.00E-07	-2.00E-07	-3.00E-06	0.198
Aug/24/2014 13:00 to					
Aug/25/2014 13:00	-1.20E-06	-4.00E-07	-2.00E-07	-3.00E-06	0.198
Aug/25/2014 13:00 to					
Aug/26/2014 13:00	-7.37E-07	-2.00E-07	-1.00E-08	-2.00E-06	0.191
Aug/26/2014 13:00 to					
Aug/27/2014 13:00	-8.00E-07	-3.00E-07	-1.00E-07	-2.00E-06	0.193
Aug/27/2014 13:00 to					
Aug/28/2014 13:00	-8.67E-07	-3.00E-07	-3.00E-07	-2.00E-06	0.180
Aug/28/2014 13:00 to					
Aug/29/2014 13:00	-3.67E-07	-3.00E-07	2.00E-07	-1.00E-06	0.169
Aug/29/2014 13:00 to					
Aug/30/2014 13:00	-1.01E-06	-1.00E-07	8.00E-08	-3.00E-06	0.168
Aug/30/2014 13:00 to					
Aug/31/2014 13:00	-1.06E-06	-1.00E-07	-9.00E-08	-3.00E-06	0.152
Aug/31/2014 13:00 to					
Sep/1/2014 13:00	-1.23E-06	-4.00E-07	-3.00E-07	-3.00E-06	0.168

Table 3: Mean, median, max, min, and R_{ns} of the Stillwater River velocity data from the south location.

Table 4: B Stream Velocity Statistics at Location 1

Time Window	Location 1				R _{nss}
	n=5 mean	median	max	min	
Jun 24 2014 1:00 to Jun 25 2014 1:00	-8.06E-06	-8.00E-06	7.00E-07	-2.00E-05	0.295
Jun 25 2014 1:00 to Jun 26 2014 1:00	-2.60E-05	-2.00E-05	-2.00E-05	-5.00E-05	0.136
Jun 26 2014 1:00 to Jun 27 2014 1:00	-4.80E-05	-3.00E-05	-2.00E-05	-9.00E-05	0.238
Jun 27 2014 1:00 to Jun 28 2014 1:00	-8.60E-06	-7.00E-06	-1.00E-06	-2.00E-05	0.507
Jun 28 2014 1:00 to Jun 29 2014 1:00	-1.36E-05	-1.00E-05	-8.00E-06	-2.00E-05	0.313
Jun 29 2014 1:00 to Jun 30 2014 1:00	-6.80E-06	-6.00E-06	-4.00E-06	-1.00E-05	0.177
Jun 30 2014 1:00 to July 1 2014 1:00	-5.40E-06	-4.00E-06	-4.00E-06	-9.00E-06	0.164
July 1 2014 1:00 to July 2 2014 1:00	-3.80E-06	-3.00E-06	-2.00E-06	-7.00E-06	0.166
	n=5 mean	median	max	min	R _{nss}
July 2 2014 13:00 to July 3 2014 13:00	-1.20E-05	-1.00E-05	-1.00E-05	-2.00E-05	0.392
July 3 2014 13:00 to July 4 2014 13:00	-2.00E-05	-2.00E-05	-2.00E-05	-2.00E-05	0.233
July 4 2014 13:00 to July 5 2014 13:00	-4.00E-05	-4.00E-05	-3.00E-05	-5.00E-05	0.334
July 5 2014 13:00 to July 6 2014 13:00	1.60E-05	2.00E-05	2.00E-05	1.00E-05	0.392
July 6 2014 13:00 to July 7 2014 13:00	2.14E-05	2.00E-05	4.00E-05	8.00E-06	0.275
July 7 2014 13:00 to July 8 2014 13:00	0.00E+00	-2.00E-06	1.00E-05	-1.00E-05	0.460
July 8 2014 13:00 to July 9 2014 13:00	-2.60E-05	-3.00E-05	-2.00E-05	-3.00E-05	0.302
July 9 2014 13:00 to July 10 2014 13:00	-2.60E-05	-3.00E-05	-2.00E-05	-3.00E-05	0.469
July 10 2014 13:00 to July 11 2014 13:00	-2.20E-05	-2.00E-05	-2.00E-05	-3.00E-05	0.974
July 11 2014 13:00 to July 12 2014 13:00	-6.20E-06	-5.00E-06	4.00E-06	-2.00E-05	1.370
	n=5 mean	median	max	min	R _{nss}
Aug 1 2014 12:00 to Aug 2 2014 12:00	-2.00E-05	-2.00E-05	-1.00E-05	-3.00E-05	0.148

Table 4. Continued

Aug 2 2014 12:00 to Aug 3 2014 12:00	-2.20E-05	-2.00E-05	-2.00E-05	-3.00E-05	0.143
Aug 3 2014 12:00 to Aug 4 2014 12:00	-1.40E-05	-1.00E-05	-1.00E-05	-2.00E-05	0.150
Aug 4 2014 12:00 to Aug 5 2014 12:00	-1.60E-05	-2.00E-05	-1.00E-05	-2.00E-05	0.140
Aug 5 2014 12:00 to Aug 6 2014 12:00	-9.80E-06	-1.00E-05	-9.00E-06	-1.00E-05	0.129
Aug 6 2014 12:00 to Aug 7 2014 12:00	-2.20E-05	-3.00E-05	2.00E-05	-4.00E-05	0.225
Aug 7 2014 12:00 to Aug 8 2014 12:00	-2.20E-05	-2.00E-05	-2.00E-05	-3.00E-05	0.205
Aug 8 2014 12:00 to Aug 9 2014 12:00	-3.40E-05	-4.00E-05	2.00E-05	-7.00E-05	0.273
Aug 9 2014 12:00 to Aug 10 2014 12:00	-2.20E-05	-2.00E-05	-2.00E-05	-3.00E-05	0.216
Aug 10 2014 12:00 to Aug 11 2014 12:00	-1.30E-05	-1.00E-05	-6.00E-06	-3.00E-05	0.187
Aug 11 2014 12:00 to Aug 12 2014 12:00	-1.06E-05	-1.00E-05	-5.00E-06	-2.00E-05	0.170
Aug 12 2014 12:00 to Aug 13 2014 12:00	-9.60E-06	-8.00E-06	-5.00E-06	-2.00E-05	0.171
Aug 13 2014 12:00 to Aug 14 2014 12:00	-1.00E-05	-8.00E-06	-6.00E-06	-2.00E-05	0.184
Aug 14 2014 12:00 to Aug 15 2014 12:00	1.60E-06	3.00E-06	1.00E-05	-1.00E-05	0.504
	n=5				
	mean	median	max	min	R _{nss}
Aug 15 2014 13:00 to Aug 16 2014 13:00	-2.00E-06	-5.00E-06	6.00E-06	-1.00E-05	0.308
Aug 16 2014 13:00 to Aug 17 2014 13:00	-2.40E-05	-2.00E-05	-2.00E-05	-3.00E-05	0.230
Aug 17 2014 13:00 to Aug 18 2014 13:00	2.20E-05	3.00E-05	3.00E-05	1.00E-05	0.226
Aug 18 2014 13:00 to Aug 19 2014 13:00	-1.80E-05	-2.00E-05	-1.00E-05	-2.00E-05	0.232
Aug 19 2014 13:00 to Aug 20 2014 13:00	-2.20E-05	-2.00E-05	-2.00E-05	-3.00E-05	0.227
Aug 20 2014 13:00 to Aug 21 2014 13:00	-1.20E-05	-1.00E-05	-1.00E-05	-2.00E-05	0.196
Aug 21 2014 13:00 to Aug 22 2014 13:00	-1.60E-05	-2.00E-05	-1.00E-05	-2.00E-05	0.188
Aug 22 2014 13:00 to Aug 23 2014 13:00	-2.00E-05	-2.00E-05	-2.00E-05	-2.00E-05	0.180
Aug 23 2014 13:00 to Aug 24 2014 13:00	-1.10E-05	-9.00E-06	-8.00E-06	-2.00E-05	0.190
Aug 24 2014 13:00 to Aug 25 2014 13:00	-9.00E-06	-9.00E-06	-8.00E-06	-1.00E-05	0.168
Aug 25 2014 13:00 to Aug 26 2014 13:00	-6.60E-06	-6.00E-06	-5.00E-06	-9.00E-06	0.178
Aug 26 2014 13:00 to Aug 27 2014 13:00	-5.60E-06	-5.00E-06	-5.00E-06	-7.00E-06	0.173

Table 4. Continued

Aug 27 2014 13:00 to Aug 28 2014 13:00	-5.40E-06	-5.00E-06	-5.00E-06	-6.00E-06	0.423
Aug 28 2014 13:00 to Aug 29 2014 8:00	-6.20E-06	-6.00E-06	-3.00E-06	-9.00E-06	0.357
	n=5 mean	median	max	min	R _{nss}
Aug 29 2014 15:00 to Aug 30 2014 15:00	3.20E-06	3.00E-06	1.00E-05	-3.00E-06	0.263
Aug 30 2014 15:00 to Aug 31 2014 15:00	-1.86E-05	-1.00E-05	-1.00E-08	-6.00E-05	0.350
Aug 31 2014 15:00 to Sep 1 2014 15:00	-5.20E-05	-5.00E-05	-3.00E-05	-9.00E-05	0.275
Sep 1 2014 15:00 to Sep 2 2014 15:00	-1.40E-05	-1.00E-05	-1.00E-05	-2.00E-05	0.200
Sep 2 2014 15:00 to Sep 3 2014 15:00	-1.18E-05	-1.00E-05	-9.00E-06	-2.00E-05	0.205
Sep 3 2014 15:00 to Sep 4 2014 15:00	-9.00E-06	-1.00E-05	-7.00E-06	-1.00E-05	0.200
Sep 4 2014 15:00 to Sep 5 2014 15:00	-1.60E-05	-2.00E-05	-1.00E-05	-2.00E-05	0.195
Sep 5 2014 15:00 to Sep 6 2014 15:00	-9.20E-06	-1.00E-05	-7.00E-06	-1.00E-05	0.193
Sep 6 2014 15:00 to Sep 7 2014 15:00	-9.40E-06	-9.00E-06	-3.00E-06	-2.00E-05	0.209
Sep 7 2014 15:00 to Sep 8 2014 15:00	5.32E-06	5.00E-06	1.00E-05	6.00E-07	0.273
Sep 8 2014 15:00 to Sep 9 2014 15:00	7.80E-06	1.00E-05	1.00E-05	2.00E-06	0.239
Sep 9 2014 15:00 to Sep 10 2014 15:00	7.60E-06	9.00E-06	1.00E-05	3.00E-06	0.243
Sep 10 2014 15:00 to Sep 11 2014 15:00	2.40E-06	2.00E-06	6.00E-06	-3.00E-06	0.326
Sep 11 2014 15:00 to Sep 12 2014 10:00	2.74E-05	3.00E-05	4.00E-05	7.00E-06	0.200

Table 4: Mean, median, max, min, and R_{nss} of the B Stream velocity data from the location 1.

Table 5: B Stream Velocity Statistics at Location

Time Window	Location 2				R _{nss}
	n=2 mean	median	max	min	
Jun 24 2014 1:00 to Jun 25 2014 1:00	-2.00E-05	-2.00E-05	-2.00E-05	-2.00E-05	0.115
Jun 25 2014 1:00 to Jun 26 2014 1:00	-2.00E-05	-2.00E-05	-2.00E-05	-2.00E-05	0.014
Jun 26 2014 1:00 to Jun 27 2014 1:00	-4.00E-05	-4.00E-05	-4.00E-05	-4.00E-05	0.009
Jun 27 2014 1:00 to Jun 28 2014 1:00	-3.50E-05	-3.50E-05	-3.00E-05	-4.00E-05	0.105
Jun 28 2014 1:00 to Jun 29 2014 1:00	-2.00E-05	-2.00E-05	-2.00E-05	-2.00E-05	0.041
Jun 29 2014 1:00 to Jun 30 2014 1:00	-2.00E-05	-2.00E-05	-2.00E-05	-2.00E-05	0.018
Jun 30 2014 1:00 to July 1 2014 1:00	-1.00E-05	-1.00E-05	-1.00E-05	-1.00E-05	0.033
July 1 2014 1:00 to July 2 2014 1:00	-1.00E-05	-1.00E-05	-1.00E-05	-1.00E-05	0.030
	n=2 mean	median	max	min	R _{nss}
July 2 2014 13:00 to July 3 2014 13:00	-1.30E-05	-1.30E-05	-6.00E-06	-2.00E-05	0.336
July 3 2014 13:00 to July 4 2014 13:00	-2.00E-05	-2.00E-05	-2.00E-05	-2.00E-05	0.151
July 4 2014 13:00 to July 5 2014 13:00	-2.50E-05	-2.50E-05	-2.00E-05	-3.00E-05	0.101
July 5 2014 13:00 to July 6 2014 13:00	2.00E-05	2.00E-05	2.00E-05	2.00E-05	0.100
July 6 2014 13:00 to July 7 2014 13:00	1.50E-05	1.50E-05	2.00E-05	1.00E-05	0.356
July 7 2014 13:00 to July 8 2014 13:00	-9.50E-06	-9.50E-06	-9.00E-06	-1.00E-05	1.350
July 8 2014 13:00 to July 9 2014 13:00	-3.50E-05	-3.50E-05	-3.00E-05	-4.00E-05	1.150
July 9 2014 13:00 to July 10 2014 13:00	-5.00E-05	-5.00E-05	-4.00E-05	-6.00E-05	1.080
July 10 2014 13:00 to July 11 2014 13:00	-6.50E-05	-6.50E-05	-4.00E-05	-9.00E-05	1.300
July 11 2014 13:00 to July 12 2014 13:00	-7.00E-05	-7.00E-05	-5.00E-05	-9.00E-05	0.688
	n=5 mean	median	max	min	R _{nss}
Aug 1 2014 12:00 to Aug 2 2014 12:00	-2.00E-05	-2.00E-05	-1.00E-05	-3.00E-05	0.057

Table 5. Continued

Aug 2 2014 12:00 to Aug 3 2014 12:00	-2.40E-05	-2.00E-05	-2.00E-05	-3.00E-05	0.042
Aug 3 2014 12:00 to Aug 4 2014 12:00	-2.00E-05	-2.00E-05	-2.00E-05	-2.00E-05	0.046
Aug 4 2014 12:00 to Aug 5 2014 12:00	-1.40E-05	-1.00E-05	-1.00E-05	-2.00E-05	0.043
Aug 5 2014 12:00 to Aug 6 2014 12:00	-2.00E-05	-2.00E-05	-2.00E-05	-2.00E-05	0.061
Aug 6 2014 12:00 to Aug 7 2014 12:00	-2.40E-05	-2.00E-05	-2.00E-05	-3.00E-05	0.042
Aug 7 2014 12:00 to Aug 8 2014 12:00	-2.40E-05	-2.00E-05	-2.00E-05	-3.00E-05	0.058
Aug 8 2014 12:00 to Aug 9 2014 12:00	-3.80E-05	-3.00E-05	-3.00E-05	-6.00E-05	0.050
Aug 9 2014 12:00 to Aug 10 2014 12:00	-1.80E-05	-2.00E-05	-1.00E-05	-2.00E-05	0.060
Aug 10 2014 12:00 to Aug 11 2014 12:00	-1.60E-05	-2.00E-05	-1.00E-05	-2.00E-05	0.063
Aug 11 2014 12:00 to Aug 12 2014 12:00	-9.60E-06	-1.00E-05	-8.00E-06	-1.00E-05	0.081
Aug 12 2014 12:00 to Aug 13 2014 12:00	-8.80E-06	-1.00E-05	-6.00E-06	-1.00E-05	0.139
Aug 13 2014 12:00 to Aug 14 2014 12:00	-1.04E-05	-1.00E-05	-6.00E-06	-2.00E-05	0.149
Aug 14 2014 12:00 to Aug 15 2014 12:00	3.80E-06	6.00E-06	7.00E-06	-7.00E-06	0.516
	n=5				
	mean	median	max	min	R _{nss}
Aug 15 2014 13:00 to Aug 16 2014 13:00	-2.00E-05	-2.00E-05	-1.00E-05	-3.00E-05	0.034
Aug 16 2014 13:00 to Aug 17 2014 13:00	-3.40E-05	-3.00E-05	-3.00E-05	-4.00E-05	0.026
Aug 17 2014 13:00 to Aug 18 2014 13:00	-5.40E-05	-7.00E-05	4.00E-05	-9.00E-05	0.154
Aug 18 2014 13:00 to Aug 19 2014 13:00	-5.20E-05	-5.00E-05	-4.00E-05	-7.00E-05	0.087
Aug 19 2014 13:00 to Aug 20 2014 13:00	-3.60E-05	-4.00E-05	-3.00E-05	-4.00E-05	0.092
Aug 20 2014 13:00 to Aug 21 2014 13:00	-1.80E-05	-2.00E-05	-1.00E-05	-2.00E-05	0.050
Aug 21 2014 13:00 to Aug 22 2014 13:00	-1.20E-05	-1.00E-05	-1.00E-05	-2.00E-05	0.061
Aug 22 2014 13:00 to Aug 23 2014 13:00	-1.36E-05	-1.00E-05	-8.00E-06	-2.00E-05	0.072
Aug 23 2014 13:00 to Aug 24 2014 13:00	-9.00E-06	-6.00E-06	-5.00E-06	-2.00E-05	0.079
Aug 24 2014 13:00 to Aug 25 2014 13:00	-6.60E-06	-6.00E-06	-5.00E-06	-1.00E-05	0.096
Aug 25 2014 13:00 to Aug 26 2014 13:00	-5.60E-06	-5.00E-06	-4.00E-06	-1.00E-05	0.087
Aug 26 2014 13:00 to Aug 27 2014 13:00	-4.80E-06	-4.00E-06	-3.00E-06	-8.00E-06	0.082

Table 5. Continued

Aug 27 2014 13:00 to Aug 28 2014 13:00	-4.40E-06	-4.00E-06	-4.00E-06	-6.00E-06	0.075
Aug 28 2014 13:00 to Aug 29 2014 8:00	-3.20E-06	-3.00E-06	-2.00E-06	-6.00E-06	0.070
	n=5 mean	median	max	min	R_{nss}
Aug 29 2014 15:00 to Aug 30 2014 15:00	-1.00E-05	-8.00E-06	5.00E-06	-3.00E-05	0.069
Aug 30 2014 15:00 to Aug 31 2014 15:00	-6.20E-05	-6.00E-05	-2.00E-05	-9.00E-05	0.199
Aug 31 2014 15:00 to Sep 1 2014 15:00	-7.20E-05	-7.00E-05	-5.00E-05	-9.00E-05	0.070
Sep 1 2014 15:00 to Sep 2 2014 15:00	-2.20E-05	-2.00E-05	-2.00E-05	-3.00E-05	0.024
Sep 2 2014 15:00 to Sep 3 2014 15:00	-1.80E-05	-2.00E-05	-1.00E-05	-2.00E-05	0.025
Sep 3 2014 15:00 to Sep 4 2014 15:00	-1.00E-05	-1.00E-05	-1.00E-05	-1.00E-05	0.038
Sep 4 2014 15:00 to Sep 5 2014 15:00	-1.56E-05	-2.00E-05	-8.00E-06	-2.00E-05	0.038
Sep 5 2014 15:00 to Sep 6 2014 15:00	-8.20E-06	-9.00E-06	-6.00E-06	-1.00E-05	0.034
Sep 6 2014 15:00 to Sep 7 2014 15:00	-8.60E-06	-9.00E-06	-1.00E-06	-2.00E-05	0.044
Sep 7 2014 15:00 to Sep 8 2014 15:00	-3.80E-06	-5.00E-06	9.00E-06	-1.00E-05	0.071
Sep 8 2014 15:00 to Sep 9 2014 15:00	7.80E-06	7.00E-06	2.00E-05	-1.00E-06	0.084
Sep 9 2014 15:00 to Sep 10 2014 15:00	-6.20E-06	4.00E-06	9.00E-06	-4.00E-05	0.104
Sep 10 2014 15:00 to Sep 11 2014 15:00	-2.20E-05	-7.00E-06	1.00E-06	-5.00E-05	0.161
Sep 11 2014 15:00 to Sep 12 2014 10:00	3.80E-05	4.00E-05	5.00E-05	2.00E-05	0.060

Table 5: Mean, median, max, min, and R_{nss} of the B Stream velocity data from the location 2.

BIOGRAPHY OF THE AUTHOR

Jarrold Cicha was born in Maplewood, Minnesota in 1991 to his parents, Doug and Lisa. He grew up in East Bethel and Isanti, Minnesota and graduated from Cambridge-Isanti High School in 2009. He continued his education at the University Of Minnesota Morris and graduated with his B.A. in Geology and B.A. in Environmental Science in August of 2013. After receiving his undergraduate degrees he began his time at The University of Maine. During his time at The University of Maine, Jarrod attended and spoke at three conferences (Maine Water Conference, The Geological Society of Maine Fall Meeting, and North East GSA). He is a candidate for the Master of Science degree in Earth and Climate Sciences from the University of Maine in August 2015.